



Review

Insight of magnesium alloys and composites for orthopedic implant applications – a review

R Radha *, D Sreekanth

School of Mechanical and Building Sciences, VIT University, Chennai, India

Received 17 March 2017; revised 28 July 2017; accepted 14 August 2017

Available online

Abstract

Magnesium (Mg) and its alloys have been widely researched for orthopedic applications recently. Mg alloys have stupendous advantages over the commercially available stainless steel, Co-Cr-Ni alloy and titanium implants. Till date, extensive mechanical, in-vitro and in-vivo studies have been done to improve the biomedical performance of Mg alloys through alloying, processing conditions, surface modification etc. This review comprehensively describes the strategies for improving the mechanical and degradation performance of Mg alloys through properly tailoring the composition of alloying elements, reinforcements and processing techniques. It also highlights the status and progress of research in to (i) the selection of nutrient elements for alloying, reinforcement and its effects (ii) type of Mg alloy system (binary, ternary and quaternary) and composites (iii) grain refinement for strengthening through severe plastic deformation techniques. Furthermore it also emphasizes on the importance of Mg composites with regard to hard tissue applications.

© 2017 Production and hosting by Elsevier B.V. on behalf of Chongqing University. This is an open access article under the CC BY-NC-ND license (<http://creativecommons.org/licenses/by-nc-nd/4.0/>).

Keywords: Orthopedic implants; Magnesium; Alloy system; Composites; Grain refinement; Processing, degradation, strengthening

1. Introduction

Orthopedic surgery in recent times depends profoundly on the development of biomaterials used for fixation of fractures and joint replacement. Biomaterials contribute significantly to the improvement of the health and well-being of humankind. The human bodies are often susceptible to painful and disabling injuries such as strains, sprains, dislocation and fractures. Fractures are simply a break in bone which is caused by the forces that exceed the strength of osseous tissue in the bone. The risk of fracture is affected by age, gender, and bone strength and pre-existing medical conditions apart from accidents. Most fractures are caused by excessive external forces and are classified as traumatic fractures. Orthopedic biomaterials can be implanted in to or near a bone fracture to facilitate healing or to compensate for a lack or loss of bone tissue. The ends of the fractured bone may be fixed in place by metal pins connected to an external frame; once the fracture has healed, the pins and frame are removed. In other cases, an operation is performed to

open up the injury site and fasten together the bone pieces with metal screws, nails, plates, rods or wires. These implants are generally left in the body even after the bone has healed which may lead to infections caused by the degradation of the implant in the physiological environment. This is of the major interest in the development of orthopedic implant with the good corrosion resistance and adaptations to biological environments. Besides this, the implant material has to have sufficient mechanical strength to withstand various biomechanical forces. The mechanical properties of interest for an implant material are yield strength, elastic modulus and ultimate tensile strength for load bearing applications. Other properties which are expected in implant materials are low weight, good wear resistance and osseointegration. The use of increasing number of orthopedic devices such as joint prostheses and internal fixations helps in increasing the expectancy of human life span. Explorations in the biodegradable materials are required to enhance device performance, to improve function, deliver bioactive compounds and achieve the goal of tissue regeneration. There are mainly three kinds of biological implant materials: metallic materials, ceramic materials and polymeric materials. Owing to their mechanical strength, metallic materials have been widely used in orthopedic applications of which commonly used are:

* Corresponding author. School of Mechanical and Building Sciences, VIT University, Chennai, India

E-mail address: radha8vit@gmail.com (R. Radha).

<http://dx.doi.org/10.1016/j.jma.2017.08.003>

2213-9567/© 2017 Production and hosting by Elsevier B.V. on behalf of Chongqing University. This is an open access article under the CC BY-NC-ND license (<http://creativecommons.org/licenses/by-nc-nd/4.0/>).

stainless steel, cobalt-chromium alloy and titanium alloy etc. The development of metallic biomaterials has gained interest and their advantages and disadvantages are outlined in Table 1. However, the biggest drawback is the non-degradability of these materials in the body environment which demands the secondary surgical procedure for the removal of implants after the bone heals. Therefore, at present, great amount of research is focused on developing biodegradable, low density and highly bioactive implants without compromising on strength. One such material which meets these requirements is Mg and its alloys. The research on biodegradable implant metal materials was born at the right moment. In the 1930s, magnesium alloy has been found biodegradable in the human body. Therefore, magnesium alloys become the study hot-spot in the field of medical implant materials. Compared with biodegradable polymer material, magnesium alloys have good mechanical compatibility, and can provide higher initial stability and initial support. Their modulus and density approach the human bones. As implant materials, they can reduce the shielding of implants. They are also lighter than other medical metal. But they are difficult to process, corrode rapidly, need a better biocompatibility. This review aims to provide a comprehensive description on the research status of Mg alloys and Mg based composites targeted for orthopedic applications. This is followed by the generic design rules entailed for developing the orthopedic biomaterials in terms of biocompatibility, mechanical characteristics, ease of processing and cost factor. The effect of alloying elements and reinforcements on the mechanical/biodegradation performance on Mg alloys and Mg based composites are discoursed in detail. Finally, the critical challenges and difficulties are summarized with importance on the promising research on Mg based materials for implant applications.

2. Evolution of metallic implants

Metallic materials have a drastic growth in orthopedic surgery intended for development of orthopedic devices, including permanent implants (total joint replacement, hip prosthesis etc.) and temporary implants (pins, bone plates, screws etc.) [1]. The potency of Mg as biodegradable implant has existed for more than a century [2]. To serve as biomaterials in vivo, magnesium and its alloys should have good biocompatibility. Mg²⁺, is an essential nutrient for life and is the fourth most abundant element present in the human body [3–7]. Mg/Mg alloys are beneficial over the present-day implant materials viz. Stainless steel, Co-Cr alloys and Titanium are outlined in Table 2 [5,8–14]. The surface response of commercially available AZ91 and AZ31 alloys in Hank's solution are investigated intended to use for clinical applications [15]. The rapid corrosion of Mg associated with the release of Hydrogen (H₂) gas was observed in few studies in mid of last century inhibits the idea of using Mg. However, the research was kindled in the early 2000s, with the better understanding of corrosion kinetics in Mg. The strategies are developed to control the degradation of Mg provided the healing of fractures without the need of removal of implant by secondary surgery. The research of biodegradable Mg based materials is evolving to design the implants intended for orthopedic applications. Mg and its alloys should have good biocompatibility to serve as biomaterials. The uncertain toxicity of commercial Mg alloying elements has a potential threat that may exasperate the application of such alloys in the biomaterial field. The major drawbacks of Mg must be overcome are listed in Table 3 [10,16,17]. In this circumstance, utmost care in selection of biocompatible elements, optimized composition design for new biodegradable Mg alloys with desired bio-mechanical properties and feasible processing

Table 1
Metallic materials advantages, disadvantages and applications.

Materials	Advantages	Disadvantages	Applications
316L Stainless steel	Easily available and Low cost Excellent fabrication properties Accepted Biocompatibility and toughness	High modulus Poor corrosion resistance Poor wear resistance Allergic reaction in surrounding tissue Stress shielding effect	Bone Plates, Bone screws and pins, Wires etc.
Co-Cr alloys	Superior in terms of resistance to corrosion, fatigue and wear. High strength Long term biocompatibility	Expensive Quite difficult to machine Stress shielding effect High Modulus Biological toxicity due to Co, Cr and Ni ions release.	Shorter term implants-Bone plates and wires, Total hip replacements (THR)-Stem or hard-on-hard bearing system
Ti alloys	Excellent resistance to corrosion Lower Modulus Stronger than stainless steels Light weight Biocompatible	Poor wear resistance Poor bending ductility Expensive	Fracture Fixation plates, Fasteners, nails, rods, screws and wires, Femoral hip stems, Total Joint Replacement (TJR) arthroplasty-hips and knees.
Mg alloys	Biocompatible Biodegradable Bioresorbable Similar density and young's modulus of bone (E = 10–30GPa) Less stress shielding effect Light weight	Hydrogen evolution during degradation Less resistance to corrosion	Bone screws, Bone plates, bone pins etc.

Table 2
Key benefits of Mg.

Benefits	Characteristics	Details
Low density	Low	Mg density (1.738 g/cm ³) [8] is close to that of cortical bone (1.75–2.1 g/cm ³) [9].
High specific strength	High	strength-to-weight ratio of approximately 130 kNm/kg
High damping capacity	High	Mg has the ability to absorb energy of any metal can be used for load bearing applications [10]
Machinability and dimensional accuracy	High	Mg is the easiest structural metal to machine, and stable final dimensions are easy to achieve [11]. Consequently, complex shapes are easily producible, which is crucial for the often intricate shapes that are required for medical applications [12–14]
Stress shielding	Less	stress-shielding-related problems can be greatly reduced for many orthopaedic implants as Mg density is very close to that of bone,
Biocompatibility	Good	Mg is considered biocompatible and has been shown to increase the rate of bone formation [5]
Degradation	Good	corrosion of Mg in the body would eventually result in complete degradation and it would be beneficial for patients have temporary exposure to an implant in the body.

Table 3
Major draw backs of Mg.

Draw backs	Characteristics	Details
Elastic modulus	Low	Lower elastic modulus of Mg may be beneficial with respect to stress shielding and it is vital to ensure that any implant is designed to sustain its load without deformation [16].
Degradation	Rapid	Mg implants are intended to completely degrade, but at a slow rate to the pace of bone remodelling.
Hydrogen evolution	high	The released H ₂ gas accumulates at the surrounding soft tissues at severe degradation rate [17]. The hydrogen evolution rates for various Mg alloys containing Zn, Al and Mn are reported as 0.01 ml/cm ² /day [10].

techniques to ensure the defect free products are vital to serve efficiently.

3. Strategies for improving the mechanical and degradation performance

Magnesium has poor strength in as cast condition with high degradation rate. The strengthening of properties can be achieved through proper alloying and processing conditions. The alloying elements in self-resorbable Mg alloys should be selected not only on the improvement of mechanical properties, but also on the consideration of degradation and biocompatibility. The grain refinement and solid solution strengthening mechanism of alloying elements promotes strength improvement in magnesium. Commonly, alloying elements impart to strengthen the mechanical properties by solid-solution strengthening, precipitation hardening, and grain-refinement. The strengthening of matrix can be obtained by the addition of alloying elements which has higher solubility limit. The solid solutions can be assured with the hexagonal close-packed (HCP) structure of magnesium when alloying elements are added. Grain refinement is effectual approach to improve the mechanical properties and corrosion resistance of Mg-based alloys. Grain size strengthening is depicted by the known Hall-Petch relation $\sigma = \sigma_0 + kd^{-1/2}$ where σ is the yield strength, σ_0 is the material constant, k is the strengthening coefficient and d is the average grain diameter. The processing conditions such as casting, powder metallurgy, and other severe plastic deformation processes are highly influencing phenomenon for the grain refinement and strengthening of matrix.

4. Design of magnesium and its alloys for orthopedic application

The selection of alloying elements in biodegradable Mg alloys should be based on the biocompatibility and

improvement of mechanical properties. The addition of alloying elements can improve the strength of Mg by means of solid solution strengthening and grain refinement. The most common alloying elements utilized in biodegradable Mg alloys and their effects on properties are presented in Table 4 [18,19]. The development of biocompatible Mg alloys based on toxicity, strengthening ability and degradation rate is shown in Fig. 1.

4.1. Biocompatibility

The corrosion products of the alloys should be non-toxic and can be easily absorbed and dissolved by the surrounding tissues and excreted [20]. Elements can be classified as toxic elements, allergic elements and nutrient elements present in the human body [21–23].

- 1) Toxic elements: Cd, Be, Pb, Ba, Th
- 2) Allergic elements : Al, Co, V, Cr, Ni, Ce, La, Cu, Pr
- 3) Nutrient elements: Ca, Mn, Zn, Sn, Sr.

4.1.1. Role of alloying elements of Mg in human body

Magnesium is one of the seven essential macro minerals required for a healthy body. For any healthy adult body, 320–420 mg of magnesium is needed daily. There are about 19 mg of Mg in the average 70 kg adult body of which approximately 65% is found in the bone and teeth and the rest is distributed between the blood, body fluids, organs and other tissues. Mg is the lightest metallic material with a density of 1.738 g/cm³ and has an excellent combination of properties which includes good strength to weight ratio, fatigue and impact strength and has excellent biocompatibility. The elastic modulus of magnesium (41–45 GPa) is closer to that of natural bone (3–20 GPa) than that of iron (~211.4 GPa) or zinc (~90 GPa) [24,25]. The mismatch of elastic modulus can lead to the implant carrying a greater portion of the load and cause stress shielding of the

Table 4
Effect of alloying elements in biodegradable Mg alloys [18,19].

Alloying element	Mechanical properties	Pathophysiology	Toxicology
Ca	Improve corrosion resistance and Grain refinement	Mainly stored in bones and teeth. Blood serum level 0.919–0.993 mg/L	Metabolic disorder
Zn	Improves yield stress, reduce hydrogen gas evolution during bio-corrosion	Blood serum level 12.4–17.4 $\mu\text{mol/L}$ Essential to enzyme and immune system	Neuro toxic and hinder bone development.
Mn	Improve corrosion resistance	Blood serum level <0.8 $\mu\text{g/L}$ Influences cellular functions/immune system, bone growth	Neurological disorder
Sr	Increase bone mass and reduce the incidence of fractures. Improves corrosion resistance and grain refinement	140 mg in the human body 99% located in the bones.	Neurological disorder
Sn	Improves compressive strength and corrosion resistance	9–140 $\mu\text{g/L}$, located in higher levels in liver and less toxic	Carcinogenic
Ag	Improves tensile strength Less corrosion resistance Antibacterial effect	Blood serum level 11–26 $\mu\text{g/L}$	Uncertain

bone [26]. This biomedical incompatibility can result in critical clinical issues such as early implant loosening, damage to the healing process, skeleton thickening, and chronic inflammation [27]. Moreover, magnesium implants have been proven to stimulate the formation of new bone when they are implanted as bone fixtures [28]. The extensive applications of Mg-based alloys are still inhibited mainly by their high degradation rates and consequent loss in mechanical integrity at pH levels between 7.4 and 7.6 and high chloride environments of the physiological systems. Moreover, the rapid formation of hydrogen gas bubbles, usually within the first week after surgery, could be a negative effect of Mg-based implant [20]. Even though magnesium favors for the implant applications, faster corrosion rate and hydrogen evolution are still a major concern. Mg and its alloys, possessing high specific strength, specific stiffness, a modulus similar to human bones, and unique biodegradation, are drawing more and more interest for the application of biodegradable materials. Alloying and surface treatment of Mg alloys helps in reducing the degradation rate until the complete healing of fractured bones. Along with calcium and zinc, it is an important micro-mineral responsible for around 300 biochemical reactions in the human body. Multiple studies suggested that calcium, buoyed by magnesium enhances bone mineral density. The essential and most keen alloying nutritional elements are calcium (Ca), zinc (Zn), man-

ganese (Mn), and strontium (Sr). The main part of this review is focused on the mechanical and corrosion behavior of nutritional elements alloying with Mg.

4.1.2. Role of calcium (Ca)

Calcium plays a vital role within the body and has numerous essential functions. Bone is formed from a complex matrix of proteins within which calcium and other minerals are deposited. Bones contain 99.5% of the total calcium in your body. Calcium, phosphate and magnesium are the most important and abundant minerals in bone, with calcium and phosphate combining together in the crystalline complex; hydroxyapatite $[\text{Ca}_{10}(\text{PO}_4)_6(\text{OH})_2]$. This complex provides the hard and rigid structure of bone which is essential to its function in supporting soft tissues and as a store of calcium for other body functions. Calcium is essential for maintaining the necessary level of bone mass to support the structures of the body. It is a relatively soft metal and it is malleable and ductile. It belongs to the group 2 of the periodic table. The solubility of Ca in Mg is limited to 1.34% under equilibrium conditions. Ca helps in refining the microstructure and improves the strength and creep properties of Mg due to the formation of stable intermetallic phases. However, the intermetallic phases are brittle which initiates cracking to occur and accelerates the degradation due to galvanic corrosion. Ca is a biofunctional element and the acceptability level of biocompatibility when addition of Ca to Mg alloys is ≤ 1 wt%.

4.1.3. Role of zinc (Zn)

Zinc is one of the most essential nutrient elements in the human body and more than 85% of Zn is present in the muscles and bones. The daily requirement of Zn in the human body is found to be 15 mg. The solubility of Zn in Mg is about 6.2 wt%. It provides solid solution strengthening and ageing strengthening effect. Zinc also helps overcome the harmful corrosive effect of iron and nickel impurities that might be present in the magnesium alloy. Zn alloys show strength similar to magnesium alloys, but their density and modulus of elasticity are slightly higher which may negatively influence the healing process due to non uniform transfer of loading between implant and growing bone. It reduces hydrogen gas evolution during biocorrosion.

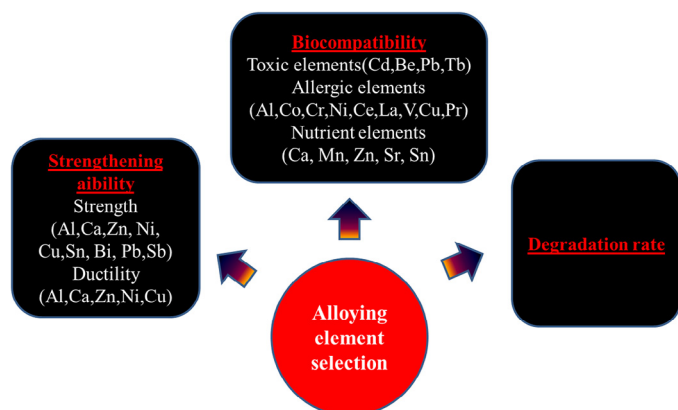


Fig. 1. Alloy design of Magnesium.

4.1.4. Role of manganese (Mn)

Manganese is an essential trace mineral in the human body beneficial for healthy bone structure, bone metabolism and helping to create enzymes for the bone formation. It helps in assisting metabolic activity in the human body. The body may contain, at most, 10–15 mg of manganese, which is concentrated mostly in the bones and the rest is distributed throughout the body in tissues like the kidneys, pancreas, liver and pituitary glands. Mn can prevent osteoporosis and it is believed to be one of the contributing factors that slow down the progress of that debilitating disease. The solubility limit of Mn in Mg is about 2.2 wt%. It helps in grain refinement and improvement in tensile strength and corrosion resistance of Mg.

4.1.5. Role of strontium (Sr)

Strontium is an important element in the human body helps and has been known to endorse the growth of osteoblasts and prevent bone resorption. Some trace elements closely chemically related to calcium, such as strontium have pharmacological effects on bone when present at levels higher than those required for normal cell physiology. The human body contains approximately 320 to 400 mg of Sr in bone and connective tissue. In addition to its antiresorptive activity, strontium was found to have anabolic activity in bone and thus may have significant beneficial effects on bone balance in normal and osteopenic animals. Accordingly, strontium has been thought to have potential in the treatment of osteoporosis. Because of its chemical similarity to calcium, strontium can replace calcium to some extent in various biochemical processes in the body, including replacing a small proportion of the calcium in hydroxyapatite crystals of calcified tissues such as bones and teeth. Strontium in these crystals imparts additional strength to these tissues. Strontium also appears to draw extra calcium into bone. The solubility of Sr in Mg is about 0.11 wt%. It helps in grain refinement and enhances the corrosion resistance of Mg.

4.1.6. Role of tin (Sn)

The daily intake of Sn ranges from 1–3 mg. Sn can encourage the synthesis of proteins and nucleic acids, which are crucial for the growth of growth. It also involved in biological reactions enhancing the stability of the internal body environment. Tin is not easily oxidized and resists corrosion because it is protected by an oxide film. It improves tensile strength and corrosion resistance of Mg. The solubility of Sn in Mg is about 14.5 wt%. Although tin itself is nontoxic, most tin salts are and may be carcinogenic. Actually, no specific function of any kind for tin has been identified in humans but believed to be beneficial in human health. The biological role of tin is still unknown and not defined.

4.2. Strengthening ability

The contribution of alloying elements to improve the mechanical properties is one of the major concerns. Al, Ca, Zn, Ni, Cu can increase the strength and ductility concurrently. Some elements like Sn, Bi, Pb, Sb favor the strength of magnesium but

Table 5

Solubility limits of nutrient elements in Mg.

Element	Solubility limits (wt %)
Sr	0.11
Ca	1.35
Mn	2.2
Zn	6.2
Sn	14.5
Ag	15.14

deteriorate the ductility. The addition of Fe, Ni, Co, Cu is to be avoided plausibly which are considered as impurities [29,30]. The impurities in Mg-based alloys can be properly controlled or else it causes toxic effects in the human body during the degradation of implant. The presence of impurities deteriorates the mechanical integrity of Mg alloys by forming secondary phases when it is reacted with alloying elements [31].

4.3. Degradation rate

Mg alloys can be used as a weight-bearing implant requires that the material should have sufficient strength not only at the moment of being implanted but also when the alloy degrades over the time while remaining in contact with body fluids. It is important that implants keep their strength at least until the bone heals. For this reason different studies have been carried out to evaluate the mass loss and evolution of the strength over the implantation or immersion time. For tuning efficiently the composition and microstructure it is first necessary to understand two of the most common types of corrosion that Mg and Mg alloys exhibit are galvanic and pitting corrosion. Galvanic corrosion develops because magnesium almost always behaves anodically in contact with other metals. Galvanic couples are usually encountered when the concentration of the alloying element surpasses their corresponding maximum solid solubility in magnesium. The extent of the galvanic effect depends on a number of factors such as the crystal orientation of the magnesium matrix, the type of secondary phases and impurity particles, the solution in which the alloy is immersed and the grain size. The concentration and distribution of secondary phases is also important for the corrosion behavior. A fine and continuous distribution of secondary phases typically improves the corrosion performance. The alloying elements and other formed intermetallic phases with close electrochemical potential to magnesium (−2.37 V) can improve the corrosion resistance by reducing the internal galvanic corrosion. The element which has low solubility limit in magnesium acts as the cathodic sites to induce corrosion which are very detrimental [32]. The solubility limits of main alloying elements are given in Table 5.

5. General processing methods of biodegradable Mg alloys

The properties of Mg based materials mainly depend on the processing techniques. Primary processing of biodegradable Mg alloys are classified as solid state and liquid state techniques. Powder metallurgy is the solid state synthesis technique

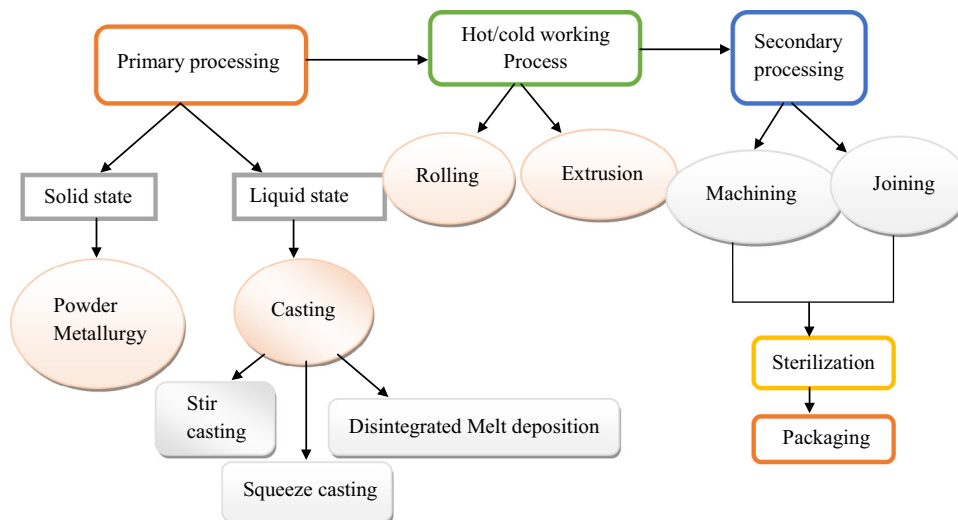


Fig. 2. Flow chart of processing sequences of biodegradable Mg alloys.

by blending the metal powders for the desired composition, compaction followed by sintering the material below its solidus temperature found to be expensive. Casting is the most economic method of processing Mg based materials by super heating in a furnace above 750 °C in an inert gas atmosphere to protect from oxidation followed by transferring the metal to the mold and allowed to solidify. The processing sequences of biodegradable Mg and its alloys from raw materials to the final medical devices are extremely important which is schematically shown in Fig. 2. The castings are subjected to hot or cold working process to get the desired form such as plates, rods, wires, and tubes. The secondary processing like machining, joining, sterilization, and packaging may be applied as needed to produce the implants.

6. Recent trends in binary, ternary, quaternary Mg alloy system and secondary processing techniques

6.1. Binary Mg alloy system

The binary Mg alloys such as Mg-Ca [33], Mg-Zn [34], Mg-Sr [35] etc., have been investigated. It was observed that yield strength was less than 150 MPa and degradation rate higher than 2 mm/year. These binary Mg alloys have been primarily examined to identify the most favorable composition in developing multi elementary Mg-based alloys and composites with superior performance for orthopedic implant applications. Mg-Ca alloys have extensively researched with varying compositions ranging from 1% to 20% for biomedical applications. The higher concentrations of Ca (5%, 10% and 20%) in Mg are found to be more brittle. The lower Ca contents (1 wt. %, 2 wt. %, and 3 wt. %) could be suitable for designing Mg-Ca alloys for orthopedic implant applications. The favorable biocompatibility, corrosion resistance and strength were observed in Mg-1Ca alloy [36]. The biocorrosion property of Mg-Ca alloys was investigated with Ca content (0.4% to 28%) in different corrosion media [37]. The less hydrogen evolution was

observed in Mg-0.8Ca alloy [38]. The finer grain size was exhibited by the as-rolled Mg-1Ca alloy due to the continuous dynamic recrystallization. The rolling process inhibits the formation of secondary phases Mg₂Ca and dislocation along the grain boundaries [39]. A summary of mechanical properties and corrosion behavior of various Mg alloys are given in Table 6 and potentiodynamic polarization curves for various Mg-Ca alloys are shown in Fig. 3.

The increase in elastic modulus, compressive strength, hardness and decrease in ductility, corrosion resistance, biocompatibility of the cast Mg-xCa alloys with the increase of Ca (x = 0.5, 1.0, 1.5, 2.9, 5.0, 10.0, 20.0 wt %). Mg-1Ca had good biocompatibility, low corrosion rate and appreciable increase in strength, ductility and elastic modulus [45]. Mg-0.6Ca exhibited the reduction in the grain size and has highest bending strength and elastic modulus which is comparable to the human bone. It has

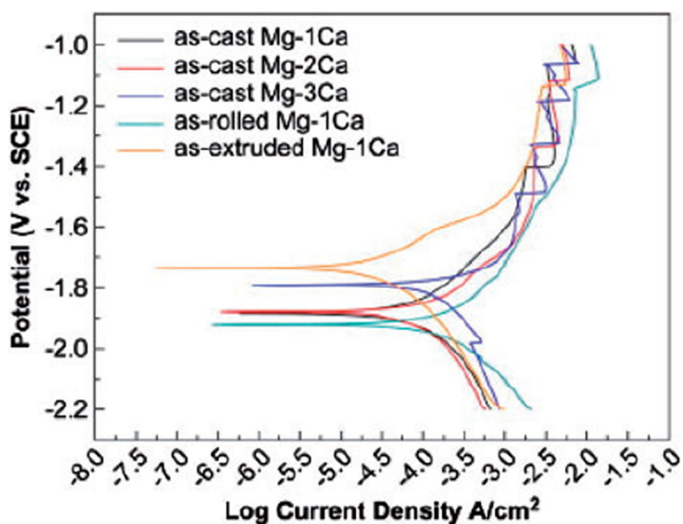


Fig. 3. Potentiodynamic polarization curves of binary Mg alloys [45].

Table 6
Mechanical and corrosion properties of Mg alloys.

Alloy	Condition	UTS (MPa)	YS (Mpa)	Hardness (HV)	Elongation (%)	Corrosion medium	In vitro (corrosion rate mm/y)	I _{corr} ($\mu\text{A}/\text{cm}^2$)	Ref
Mg	as-cast					SBF	1.94	86.06	[21]
						Hank's	0.36	15.98	[21]
	as-rolled					SBF	0.84	37.24	[21]
						Hank's	0.32	9.58	[21]
Mg-1Ca	as-cast	71.38	40		1.87	SBF	12.56	-	[33]
Mg-1Zn	as-cast	134	25.5		18.2	SBF	1.52	-	[21]
Mg-1Sn	as-cast	194	79		20	SBF	2.45	-	[21]
Mg-1Sn	Sub-rapid solidification					Hank's	0.121	5.3	[40]
Mg-3Sn							0.168	7.3	
Mg-5Sn							0.337	14.7	
Mg-7Sn							0.507	22.18	
Mg-2Sr	as-rolled	213.3	147.3		3.15	Hank's	0.87	-	[35]
Mg-1Mn	as-cast	86.3	28.5		7.5	SBF	2.46	-	[21]
Mg-1Ag	as-cast	116.2	23.5		13.2	SBF	8.12	-	[21]
Mg-2Ca	Cast	115.2	47.3	3.05	43.2	kokubo		301.9	[5]
Mg-1Ca	Cast	105	39	4.1	-	-	-	-	[41]
Mg-0.7Ca	As-cast					kokubo		$1.97\text{A}/\text{cm}^2 \times 1000$	[19]
Mg-1Ca	As-cast					kokubo		$2.24\text{ A}/\text{cm}^2 \times 1000$	[19]
Mg-2Ca	As-cast					kokubo		$3.12\text{ A}/\text{cm}^2 \times 1000$	[19]
Mg-3Ca	As-cast					kokubo		$3.95\text{ A}/\text{cm}^2 \times 1000$	[19]
Mg-4Ca	As-cast					kokubo		$4.7\text{ A}/\text{cm}^2 \times 1000$	[19]
Mg-3Ca	As-cast					SBF		$929.3\text{ }\mu\text{A}/\text{cm}^2$	[42]
RS15	As-rolled					SBF		$74.2\text{ }\mu\text{A}/\text{cm}^2$	[42]
Mg-3Ca									
RS30	As-rolled					SBF		$55.6\text{ }\mu\text{A}/\text{cm}^2$	[42]
Mg-3Ca									
RS45	As-rolled					SBF		$17.1\text{ }\mu\text{A}/\text{cm}^2$	[42]
Mg-3Ca									
Mg-0.5Sr	Homogenised + 24 h aged	74	37	2.6					[27]
Mg-1.0 Sr	Homogenised + 24 h aged	73	33	3.3					[27]
Mg-1.5Sr	Homogenised + 24 h aged	81	40	2.6					[27]
Mg-2Zn-0.5Sr	Homogenised + 24 h aged	142	62	8.9					[27]
Mg-4Zn-0.5Sr	Homogenised + 24 h aged	169	104	3					[27]
Mg-6Zn-0.5Sr	Homogenised + 24 h aged	209	128	3.6					[27]
AZ91	Slow strain rate test	106		3.5					[36]
AZ91Ca						SBF		$65.7\text{ }\mu\text{A}/\text{cm}^2$	[36]
AZ61Ca						SBF		$17.8\text{ }\mu\text{A}/\text{cm}^2$	[36]
Mg-0.5Ca						SBF (10 h)	4.08		[43]
Mg-0.5Ca						SBF (10–220 h)	2.79		[43]
Mg-1Ca						SBF (10 h)	3.2		[43]
Mg-1Ca						SBF (10–220 h)	0.66		[43]
Mg-0.5Ca-0.5Zn						SBF (10 h)	6.8		[43]
Mg-0.5Ca-0.5Zn						SBF (10–220 h)	2.3		[43]
Mg-1Ca-1Zn						SBF (10 h)	4.3		[43]
Mg-1Ca-1Zn						SBF (10–220 h)	1.6		[43]
Mg-0.5Ca-0.5Mn						SBF (10 h)	4.2		[43]
Mg-0.5Ca-0.5Mn						SBF (10–220 h)	0.83		[43]
Mg-1Ca-1Mn						SBF (10 h)	4.02		[43]
Mg-1Ca-1Mn						SBF (10–220 h)	2.82		[43]
Mg-0.5Ca-0.25Zn-0.25Mn						SBF (10 h)	6.9		[43]
Mg-0.5Ca-0.25Zn-0.25Mn						SBF (10–220 h)	0.62		[43]
Mg-1Ca-0.5Zn-0.5Mn						SBF (10 h)	4.05		[43]
Mg-1Ca-0.5Zn-0.5Mn						SBF (10–220 h)	2.09		[43]
Pure Mg		97.5	27.5	7.31	28.9	kokubo	8.47	370.7	[40]
Mg-2Ca		115.2	47.3	3.05	43.2	kokubo	6.89	301.9	[40]
Mg-4Ca		77.4	34.5	2.10	53.3	kokubo	9.04	395.7	[40]
Mg-2Ca-0.5Mn-2Zn		168.5	78.3	7.84	64.5	kokubo	1.78	78.3	[40]
Mg-2Ca-0.5Mn-4Zn		189.2	83.1	8.71	69.1	kokubo	2.27	99.6	[40]
Mg-2Ca-0.5Mn-7Zn		140.7	45.4	4.15	82.2	kokubo	3.98	174.1	[40]
Mg-1.2Zn-0.5Ca	as-cast	121.3	60.3	3.2	53	SBF	8.2	695	[44]
Mg-1.2Zn-0.5Ca	Heat treated (3 h)	150.7	84.3	4.9	62	SBF	4.8	420	[44]

high fracture deflection and less corrosion rate [46]. The microstructural, mechanical and corrosion behavior was investigated in the pure Mg and Mg–Ca alloys (up to 3 wt. % Ca). It was found that the enhancement in tensile properties, ductility and corrosion resistance in Mg alloys containing Ca greater than 1wt% after indirect type of extrusion. The disintegration of secondary phase (Mg_2Ca) along interdendritic regions occurred during extrusion was vital in improving the corrosion resistance of the Mg–Ca alloys [47]. The microstructural and corrosion behavior of cast Mg-xCa ($x = 0.5, 1.25, 2.5, 5.0, 10.0$ wt %) alloy was investigated. The amount of lamellar structure of intermetallic phases (Mg_2Ca) in the grain boundaries and the thickness of grain boundaries were noticeably increased with the addition of calcium. The increase in hardness with the increase in calcium content was observed in Mg-xCa alloy due to the precipitation of Mg_2Ca in α -Mg matrix and the grain boundary. The higher corrosion rate was observed with the increase in Ca on Mg-xCa alloy due to the presence of greater amount of Mg_2Ca surrounding the Mg dendrites. The corrosion potential E_{corr} of the specimens were more negative followed by an increase in corrosion rate, in the order of Mg-0.5Ca < Mg-1.25Ca < Mg-2.5Ca < Mg-5Ca < Mg-10Ca. The pH value was increased due to the increasing dissolution rate of Mg-xCa alloy with increasing Mg_2Ca [48]. The comparative analysis of mechanical and corrosion behavior in cast, rolled and extruded Mg-xCa alloy ($x = 1.0, 2.0, 3.0$ wt%) was investigated. The yield strength, ultimate strength and tensile strength was increased in the order of extruded Mg-xCa > rolled Mg-xCa > cast Mg-xCa alloys. The grain refinement was noticed with the increase of Ca and it is significantly improved with the secondary process such as rolling and extrusion of Mg-xCa alloy. The hot rolled and extruded Mg-xCa alloys were favored for the reduction in the formation of Mg_2Ca resulted in the lower corrosion rate. Mg-1Ca alloy did not induce cytotoxicity to L929 cells and the bone formation was noticed at the third month [36]. The cytotoxicity, biocorrosion and mechanical properties was investigated in as-cast and extruded Mg-xSn alloys ($x = 1, 3, 5, 7$ wt %). It was observed the uniform distribution of smaller Mg_2Sn phase in α -Mg matrix obstructs the growth of grain size with the increase in addition of tin content. The increase in yield strength, ultimate tensile strength and the decrease in elongation was observed with increasing Sn. The corrosion resistance was better in the lower content of Sn (Mg-1Sn) due to the lesser volume of second phases Mg_2Sn in α -Mg matrix. With the higher content of Sn in Mg, corrosion resistance was declined. Mg-1Sn and Mg-3Sn did not persuade toxicity to the MG63 cells [43]. Addition of tin caused a stronger phenomenon of constitutional supercooling resulted in lessening the secondary dendrite arm spacing [40]. The biocompatibility and biodegradability of Mg-xSr ($x = 0.3, 0.5, 0.7, 1.0, 1.2, 1.5, 2, 2.5$ wt %) was investigated. The degradation rate was slower in Mg-0.5Sr and it was hasten with the increase in Sr. It was observed the formation of Sr substituted hydroxyapatite on Mg-0.5Sr which enhances the cell growth, propagation and healing around bone implants. The micro galvanic corrosion was occurred between the Mg matrix and $Mg_{17}Sr_2$ intermetallic phases accelerate the biodegradation [49]. The hardness was

increased with the addition of Ag ($x = 2, 4, 6$ wt%) in the cast Mg-xAg alloy due to the formation of Mg_4Ag β phases and it was decreased in T4 treated. The hardness of T6 treated Mg-xAg alloy gets enhanced due to the re-precipitation of β phases. The ultimate tensile strength and ductility gets enhanced with the increase in addition of Ag. The corrosion resistance was significantly improved by T4 treatment dissolved most of silver-enriched dendrites and β phases, which resulted in more homogeneous distribution of corrosion potential on the surface. Mg-6Ag showed antibacterial activity [50]. The mechanical and corrosion behavior of cast Mg-xCa ($x = 0.6, 1.2, 1.6, 2.0$ wt %) was analyzed. The highest bending strength, elastic modulus was revealed in Mg-0.6Ca alloy. The corrosion resistance was decelerated with the increase of Ca content due to the formation of more secondary phases Mg_2Ca [46]. The hot rolled Mg-2Sr alloy revealed the highest strength and the slowest corrosion rate. The in vivo results showed that the as-rolled Mg-2Sr alloy promoted bone mineralization and new bone formation without inducing any major undesirable effects [35]. The biocompatibility of cast binary Mg-1x alloys ($x = Al, Ag, In, Mn, Si, Sn, Y, Zn$ and Zr) was investigated. It was noticed the formation of Mg_2Si phase in Mg-1Si alloy because of no solubility of Si in Mg and α -Mg phase for the remaining binary Mg alloys. The yield strength and ultimate tensile strength was significantly improved with the addition of Al, Ag, In, Si, Sn, Zn or Zr individually. The decrease in strength and elongation was noticed in Mg-1Mn and Mg-1Y alloys. The noticeable increase in strength was observed abruptly in rolled Mg-1Al and Mg-1Zn alloys. The greater reduction in elongation was observed in rolled Mg-x alloys than the cast alloys. Among the alloys, the precipitation of eutectic α phase in the rolled Mg-1Al accelerated the corrosion rate. Mg-1Al, Mg-1Sn and Mg-1Zn alloys showed no significant reduced cell viability to fibroblasts and Mg-1Al, Mg-1Si, Mg-1Sn, Mg-1Y, Mg-1Zn and Mg-1Zr alloy extracts indicated no significant toxicity to osteoblasts [51]. Mg-xSn (1, 3, 5, 7 wt%) were prepared by sub-rapid solidification processing and corrosion tests revealed increase in addition of tin increases the corrosion rate [52].

6.2. Ternary Mg alloy system

Mg-5Ca and Mg-5Ca-1Zn alloys were investigated to explore the effects of micro alloying and hot extrusion on their mechanical properties and corrosion resistance. The extruded Mg-5Ca-1Zn revealed higher compressive strength of 385 MPa and no significant structural degradation even after immersion in simulated body fluid for 30 days [42]. The corrosion properties of cast and extruded Mg-5Ca-xZn ($x = 0.5, 1.0, 1.5, 3.0$) wt% was analyzed. The increase of Zn content more than 1wt% induced a remarkable reduction in hydrogen evolution with the decrease in grain size of ~ 10 μm and best corrosion resistance is achieved at 1.5–3.0 wt% of Zn. XRD and WDS map analysis revealed that the white contrast phase of $Mg_6Ca_2Zn_3$ intermetallic compound blocking the corrosion and Mg_2Ca phase with dissolved Zn was not corrosive [53]. Mg-0.3Sr-0.3Ca alloy showed a good corrosion resistance with the hydrogen evolution rates of 0.01 mL/cm²/h in SBF, and it exhibited highest

tensile and bending properties, as well as higher ductility [54]. The corrosion properties of Mg-1Zn-xCa ($x = 0.2, 0.5, 0.8, 1.0$ wt%) prepared by zone solidification technology under three different medium of NaCl solutions (0.9 wt%, 3.5 wt%) and SBF were analyzed respectively at ambient temperature. The backward extruded Mg-1Zn-0.5Ca alloys exhibited the most anti-corrosion properties in both 0.9 wt % NaCl and SBF. The addition of 1 wt% Ca significantly promoted the dynamic recrystallization results in the grain refinement of Mg alloy [55]. The hardness and corrosion behavior of cast Mg-xCa ($x = 0.5$ wt%, 1.25 wt%) and Mg-xCa-xZn ($x = 0.5, 1.5$ wt%) Ca was investigated. The reduction in grain size was observed by adding Ca and Zn. The addition of Zn resulted in the formation of $\text{Ca}_2\text{Mg}_6\text{Zn}_3$ phase in Mg-1Ca-Zn alloys along the grain boundaries was significant for the improvement in corrosion resistance. The improvement in hardness was observed with the addition of Ca due to the solid solution effect, precipitation of Mg_2Ca and reduction in grain size of α -Mg. The addition of Zn showed further increase in hardness due to the grain size reduction and precipitation of $\text{Ca}_2\text{Mg}_6\text{Zn}_3$ particles within α -Mg grains [56]. The effect of Ca on the microstructure, mechanical, corrosion properties as well as the biocompatibility of the as-cast Mg-5Zn-xCa ($x = 1, 2, 3$ wt %) alloys were investigated. The refinement in grain size was observed with the addition of Ca from 1 to 3 wt%. The yield strength was improved with the addition of Ca (1, 2 wt %) due to the distribution of ternary $\text{Ca}_2\text{Mg}_6\text{Zn}_3$ and binary Mg_2Ca phases along the grain boundaries. The increase in the volume of $\text{Ca}_2\text{Mg}_6\text{Zn}_3$ and Mg_2Ca phases in the matrix was observed with the increase of Ca content prone to the formation of more anode-cathode sites resulted in fast corrosion rate. Hemolysis rate of Mg-5Zn-1Ca in blood environment was observed as 4.07% which was below 5% did not induce toxicity to the cells and had no destructive effect on erythrocytes [57]. The effect of secondary phases and grain size on the degradation rate of cast Mg-3Zn-0.3Ca after solution treated for 24 h and 48 h at the temperature ranging from 310 °C and 450 °C was analyzed. The higher corrosion rate was seen in the heat treated sample at the higher temperature because of the enlargement in the grain size and reduction in the volume fraction of secondary phases. The balanced grain size and volume fraction of secondary phases reduced the corrosion rate which was observed in the alloy treated at 420 °C for 24 h [58]. The degradation behavior on cast ternary alloys Mg-xCa ($x = 0.6, 1.6$ wt%)-xZn ($x = 0.8, 1.8$ wt%) was studied from polarization and immersion tests. The grain size was reduced with the addition of 0.8wt%Zn on Mg-0.6Ca alloy than the other alloy compositions. The secondary phases (Mg_2Ca , $\text{Mg}_6\text{Ca}_2\text{Zn}_3$) are crystallized along the grain boundaries as well as in interdendritic interstices which appeared more continuous. The less corrosion rate was showed in Mg-0.6Ca-xZn ($x = 0.8, 1.8$ wt%) due to the lower volume fractions of secondary phases and decrease in the potential difference due to the enrichment of Zn in the solid solution of Mg-0.6Ca-1.8Zn alloy [41]. The corrosion resistance was higher in the ultrasonic treated Mg-3Zn-0.8Ca alloy rather than the mechanically vibrated and as-cast Mg alloy due to the grain refinement with the higher concentration of oxides [59]. The

mechanical and biodegradation properties of zone solidification and backward extruded Mg-1Zn-xSr ($x = 0.2, 0.5, 0.8, 1.0$ wt%) were analyzed. The hardness, tensile and compressive properties are enhanced significantly with the higher concentration of Sr content with the decrement in grain size. The larger amount of secondary phases is formed due to its lower solubility in Mg accelerating the corrosion rate with the Sr increment in Mg-1Zn alloys [60]. The effect of Zn content on microstructure, mechanical properties and corrosion behavior of Mg-Zn-Mn alloy was investigated. The grain size was decreased from 12 to 4 μm and the mechanical properties increased remarkably when the Zn content increased from 0 to 3 wt%. The best anti-corrosion property is obtained with 1 wt% Zn while further increase of Zn content deteriorates the corrosion property. In vivo study showed that after 18 weeks, about 54% as-cast Mg-Mn-Zn (Mg-1.2Mn-1.0Zn) implant had degraded but the degradation of magnesium did not cause any increase in serum magnesium content or any disorders of the kidney after 15-weeks post implantation. More degradation phenomena of implant (Mg-1.0Zn-0.8Mn as extruded) were observed in the marrow channel than in the cortical bone [61]. Mg-Sr and Mg-Zn-Sr alloys were solution treated at 450 °C and 360 °C for 18 hours and quenched in water. The optical microscopic images of solution treated alloys are shown in Figs. 4 and 5.

Increase in Zn content (2 wt% to 6 wt %) in Mg-0.5 Sr and increase in Sr content (0.5, 1.0, 1.5 wt %) in Mg increases the strength of alloys and exhibited reduction in grain size. Higher concentration of Zn (6 wt %) showed higher corrosion rate due to the presence of secondary intermetallic phases along the grain boundaries. Mg-0.5Sr showed lesser degradation rate [62]. The degradation and mechanical integrity of AZ91 calcium containing alloy was analyzed. The development of Al_2Ca phase and subsequent decrease in $\text{Mg}_{17}\text{Al}_{12}$ was noticed with the addition of Ca in AZ91 Mg alloy as shown in Fig. 6.

Increase in general and corrosion resistance was noticed in AZ91 alloy due to the Ca addition. The 15% reduction in ultimate tensile strength and 20% reduction in elongation to fracture were observed in the slow strain rate test in modified SBF of calcium holding magnesium alloy [63]. Ageing treatment was performed on Mg-Zn-Ca alloy for different time conditions. The optical images of degraded as-cast and heat treated Mg-Zn-Ca alloys aged at 1–10 h are shown in Fig. 7. It was reported at ageing for 2 h showed the improvement in corrosion resistance and 2–5 h showed improvement in hardness, tensile strength and yield strength [44].

6.3. Quaternary Mg alloy system

The refinement of grains occurred due to the addition of Mn and Zn to binary Mg-Ca alloys. Mg-0.5Ca-0.25Zn-0.25Mn alloy exhibited the lowest hydrogen evolution rate of 0.262 cc/cm²/day. The lowest corrosion resistance of Mg-1Ca-0.5Zn-0.5Mn was observed due to the higher Ca content and lower Zn content stabilized the MgCa_2 intermetallic phase. The grain size and hardness for the Mg-Ca based alloys are depicted in Fig. 8 [64].

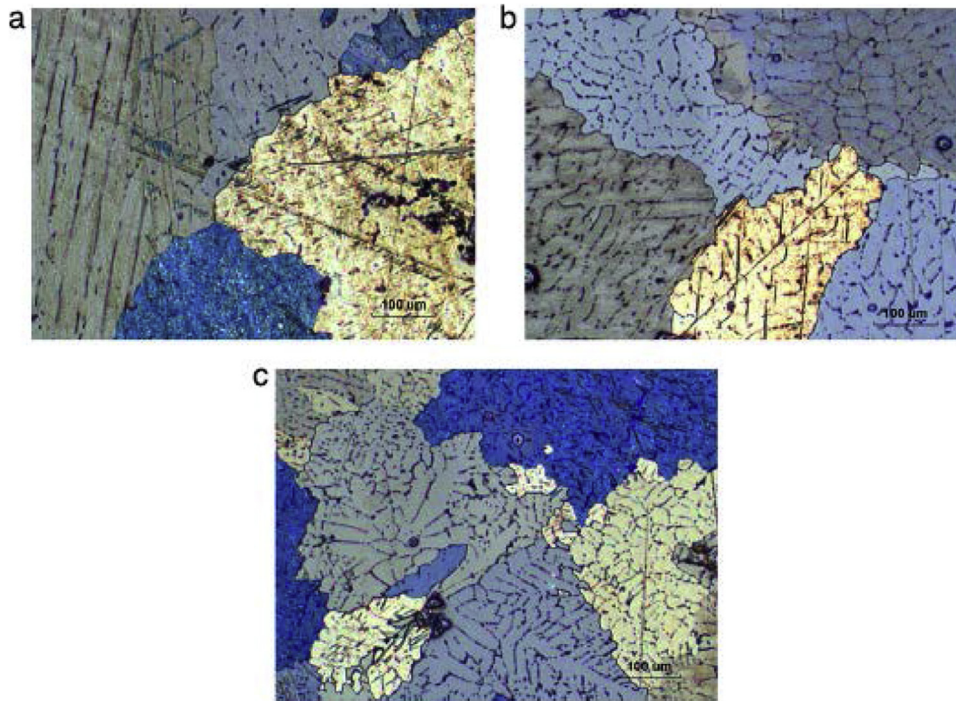


Fig. 4. Optical micrographs of solution treated alloys (a) Mg-0.5 Sr (b) Mg-1.0 Sr (c) Mg-1.5 Sr [62].

The biocorrosion and mechanical properties of Mg-2Ca-0.5Mn-xZn (2, 4, 7 wt %) was investigated. The increase in ultimate tensile strength (189.2 MPa) and elongation (8.71%) of quaternary Mg-Ca-Mn-Zn alloys was observed with increase in Zn content up to 4 wt % respectively. Grain refinement, solution strength and second phase strengthening effect

played a vital role for enhancement in tensile properties. The addition of Zn (4 wt %) in quaternary Mg alloy resulted in the precipitation of Mg_2Ca , $Mg_{12}Zn_{13}$ and $Ca_2Mg_6Zn_3$ in Mg matrix as shown in Fig. 9 which obstructs the grain growth showed remarkable improvement in hardness (69.7 Hv). However, with increase of Zn (7 wt %) deteriorated the tensile properties but

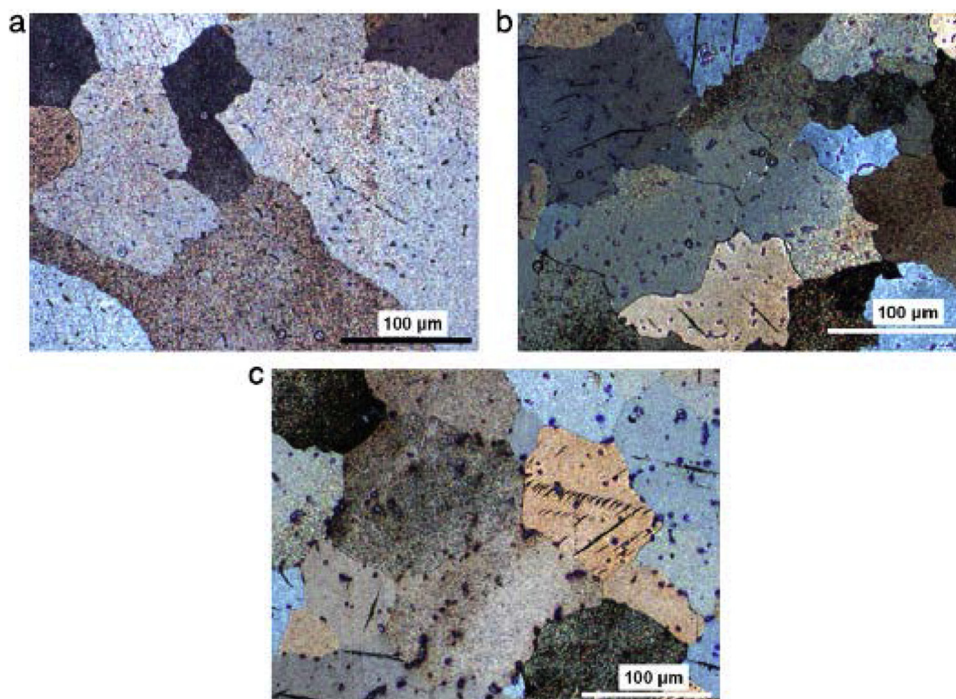


Fig. 5. Optical micrographs of solution treated alloys (a) Mg-2.0 wt% Zn-0.5 wt% Sr (b) Mg-4.0 wt% Zn-0.5 wt% Sr (c) Mg-6.0 wt% Zn-0.5 wt% Sr [62].

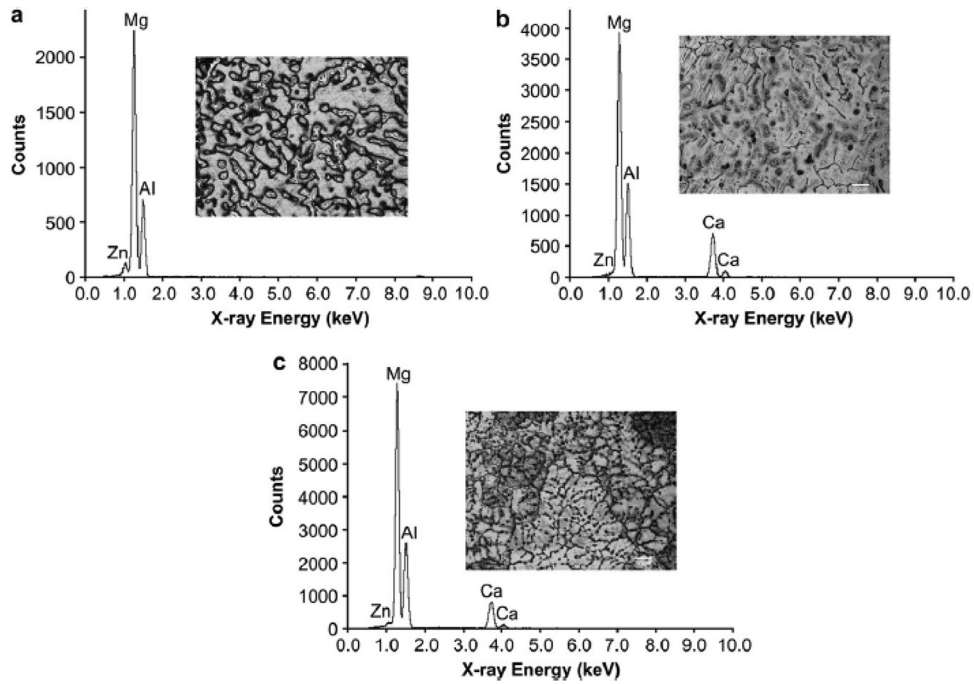


Fig. 6. An EDX spectrum of grain boundary precipitates and microstructure in: (a) AZ91, (b) AZ91Ca and (c) AZ61Ca alloys [63].

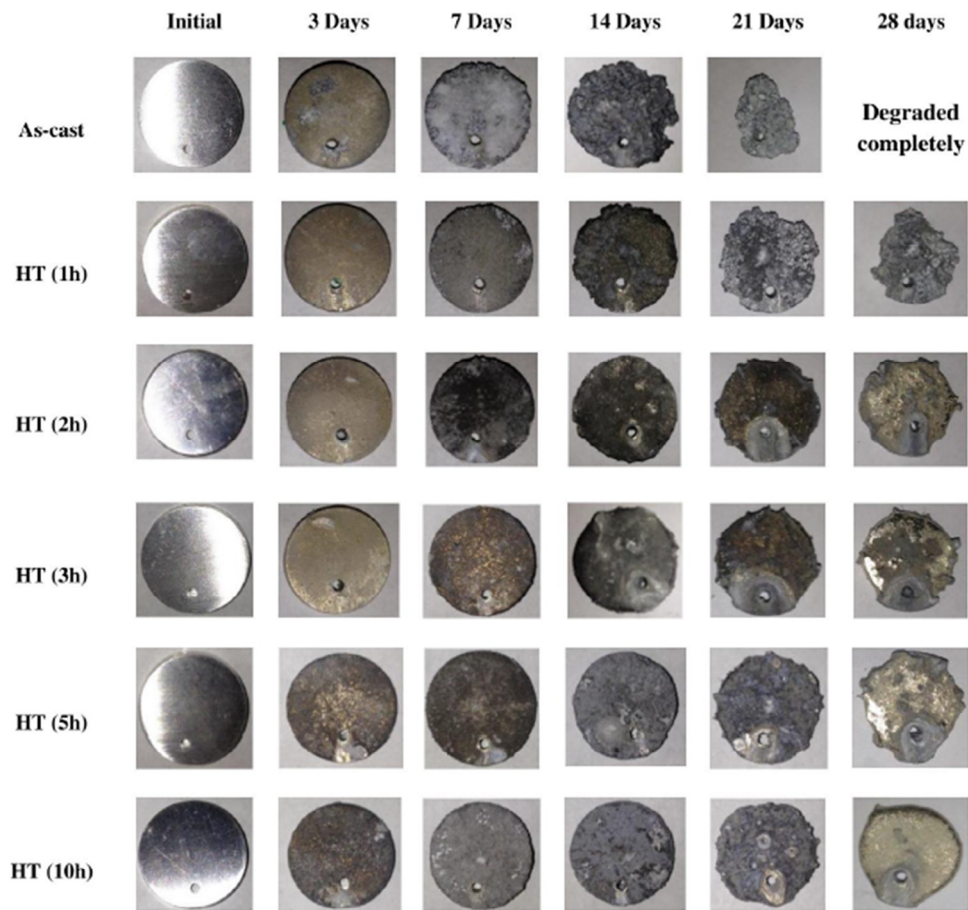


Fig. 7. optical images of degraded as-cast and heat treated Mg-Zn-Ca alloys aged at 1–10 h [44].

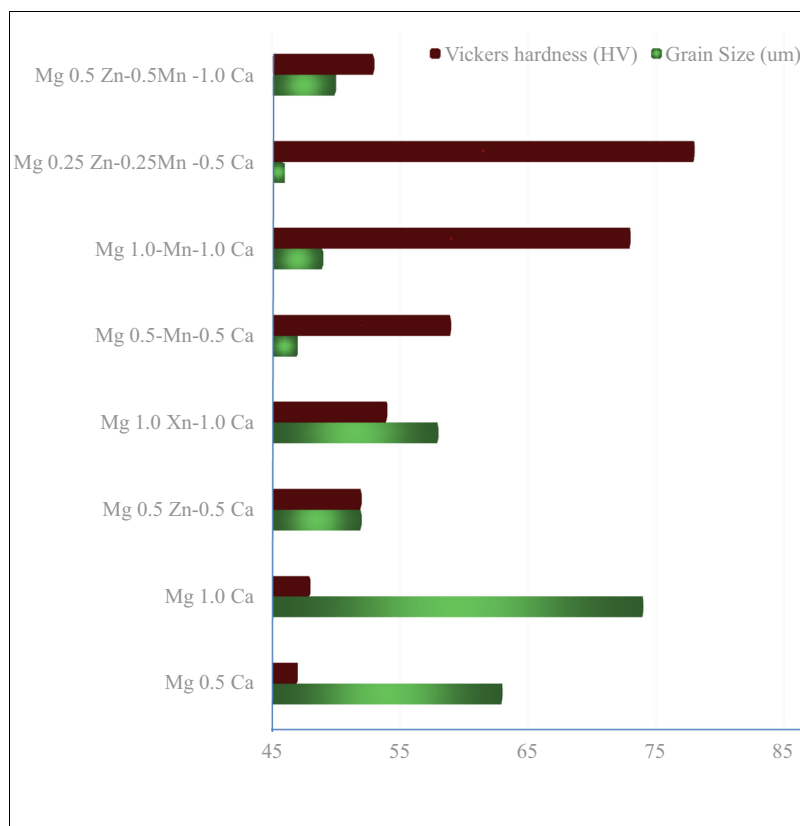


Fig. 8. Hardness and average grain size of Mg–Ca-based alloys [64].

showed the improvement in hardness (82.2 Hv). The corrosion tests in Kokubo solution revealed shift in the corrosion potential towards more noble direction due to the addition of Mn and Zn into the decreased the degradation rate of the binary Mg–Ca alloy. The lesser amounts of pit were observed in quaternary alloy system than Mg–Ca alloys [65] which is mainly linked with formation of eutectic (Mg + Mg₂Ca + Ca₂Mg₆Zn₃) phase as shown in Fig. 10.

The mechanical and biocorrosion properties of cast Mg-xZn (x = 1.8, 2.0, 1.5 wt%)-xMn (x = 1.1, 1.2, 1.1 wt%)-xCa (x = 0.3, 0.5, 1.0wt%). The secondary phases Ca₂Mg₆Zn₃ are mainly distributed along grain boundaries and a few present at interdendritic regions of inner grains as shown in Figs. 11 and 12. The grain refinement, increase in yield strength, ultimate tensile strength and elongation and corrosion resistance was observed with the calcium content of 0.3 and 0.5 wt% and results declined with the further increase of Ca content [65].

6.4. Secondary processing techniques for grain refinement of Mg alloys

The strengthening method for Mg is based on the structure design, such as grain refinement, surface modification, and with other reinforcement. The processing of Mg is intricate at ambient temperature due to its inadequate ductility. It is attributed to slip systems due to its hexagonal close-packed structure (HCP). Severe plastic deformation processes (SPD) have been adopted to improve the mechanical properties and plastic

deformation of Mg and its alloys such as equal channel angular pressing (ECAP), High pressure torsion (HPT) and extrusion. The typical microstructures of pure Mg and various Mg alloys are fabricated by different processing conditions [66–70] are illustrated in Figs. 13 and 14.

Pure Mg exhibits α (Mg) as a single phase. The equiaxed coarser grains were observed in as-cast pure Mg and finer grains were resulted by secondary deformation process such as ECAP, extrusion and rolling etc. Grain refinement becomes the main strengthening method in pure Mg. Mechanical properties of pure Mg are closely related to its microstructure, especially in grain size, and various methods have been adapted to obtain fine and homogeneous grains, including extrusion, SPD methods, and powder metallurgy methods [71–75] are given in Table 7. The effect of grain size on the degradation behavior of AZ31 magnesium alloy produced by equal channel angular pressing carried out at four passes was analyzed. The refinement in grain structure was evident when it is subjected to third and fourth passes. It was observed that lower contact angle with high surface energy enhanced the wettability of AZ31 Magnesium alloy which facilitated the strong bonding of materials with the tissues. The greater rate of mineralization was observed in the ECAP third and fourth passes samples aided to lower the degradation of AZ31 Magnesium alloy [76]. The hardness, strength and ductility, toughness of as-cast and aged Mg-3Zn alloy was improved significantly with more rolling cycles. The refinement of grains were noticed when it is

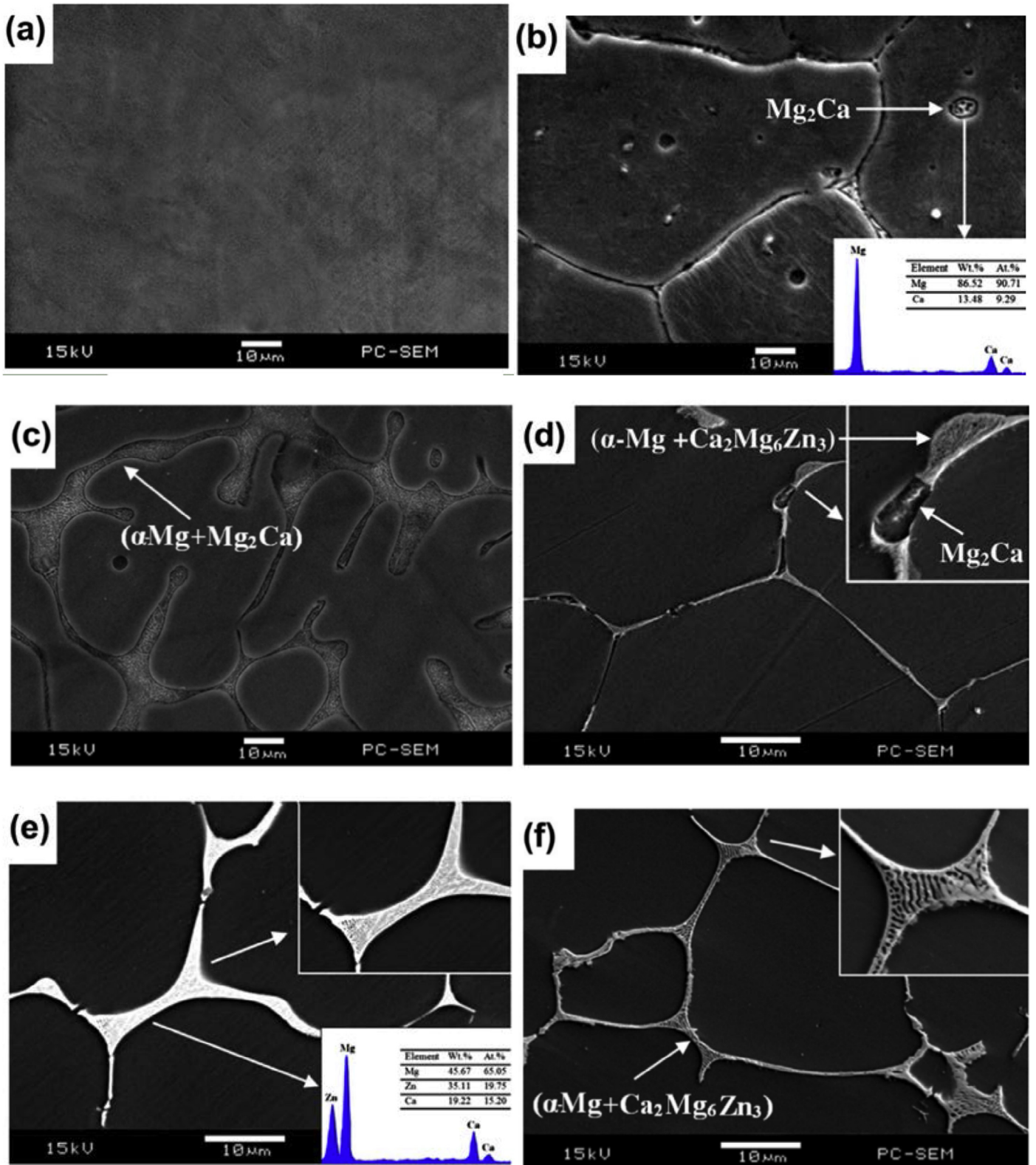


Fig. 9. SEM micrographs of (a) pure Mg (b) Mg–2Ca, (c) Mg–4Ca, (d) Mg–0.5Ca–0.5Mn–Zn alloys with various Zn content: 2 (e) 4 and (f) 7 wt.% [65].

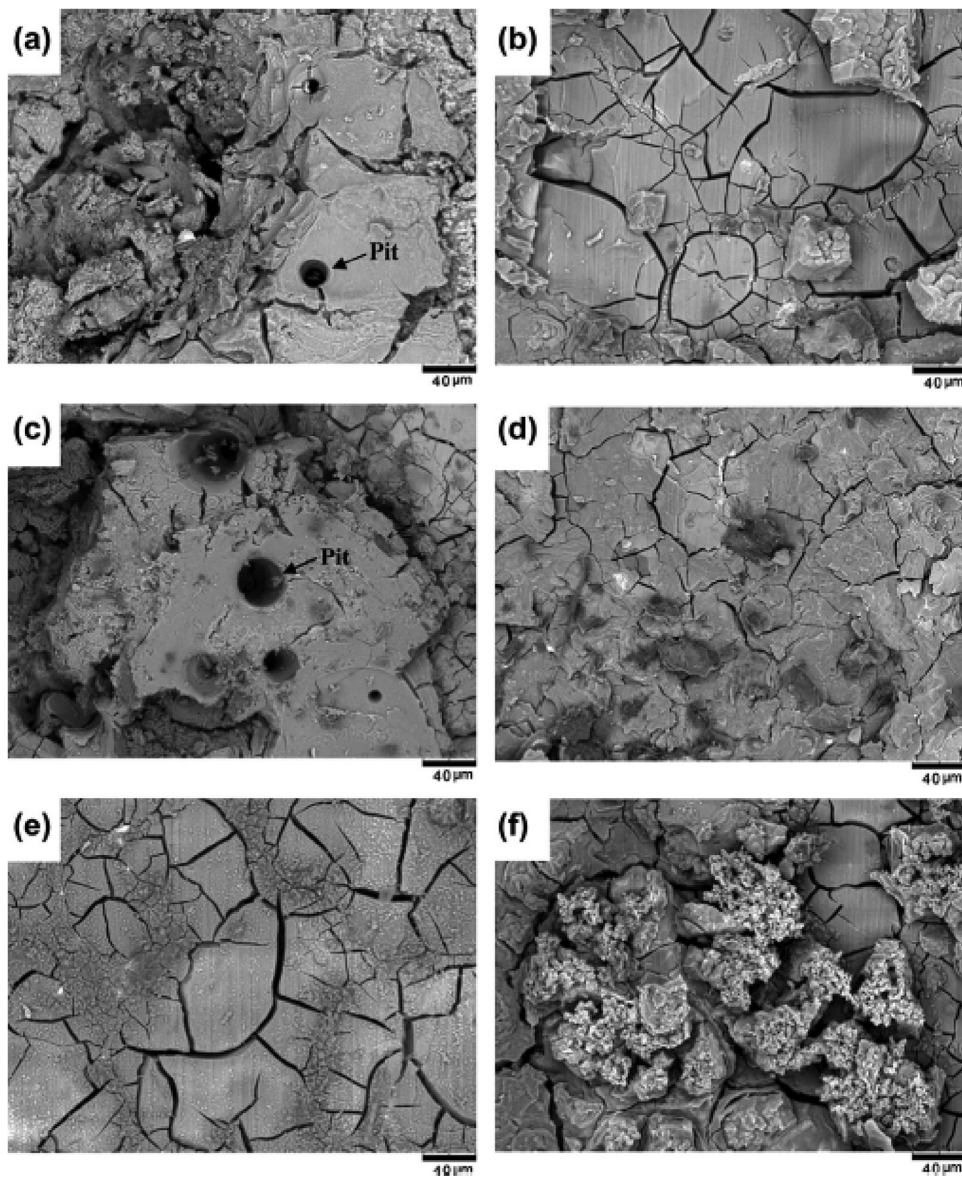


Fig. 10. SEM micrographs of (a) pure Mg (b) Mg-2Ca, (c) Mg-4Ca, (d) Mg-0.5Ca-0.5Mn-Zn alloys with various Zn content: 2 (e) 4 and (f) 7 wt.% after immersion into Kokubo solution [65].

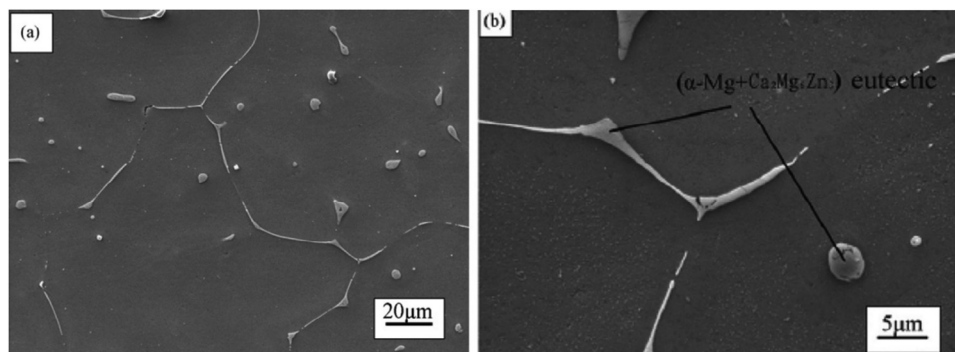


Fig. 11. (a) SEM micrographs of as-cast Mg-2Zn-1Mn-0.3Ca alloy (b) SEM morphology of the eutectic (α -Mg+Ca₂Mg₆Zn₃ + α -Mg) phase [65].

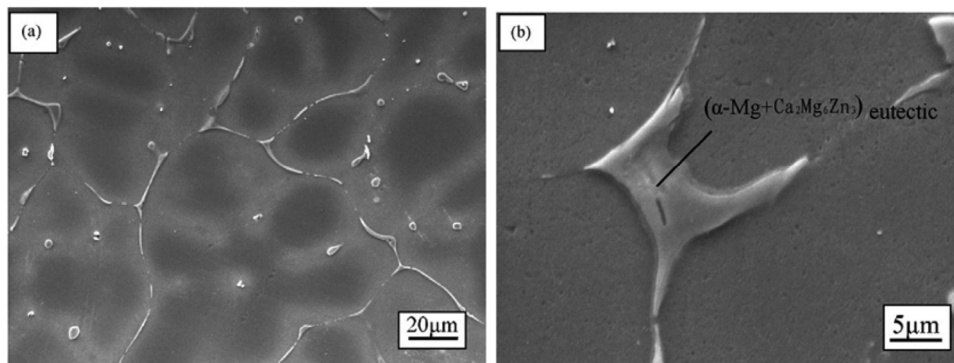


Fig. 12. SEM morphology of (a) as-cast Mg-2Zn-1Mn-0.54Ca alloy (b) eutectic ($\text{Ca}_2\text{Mg}_6\text{Zn}_3 + \alpha\text{-Mg}$) phase [65].

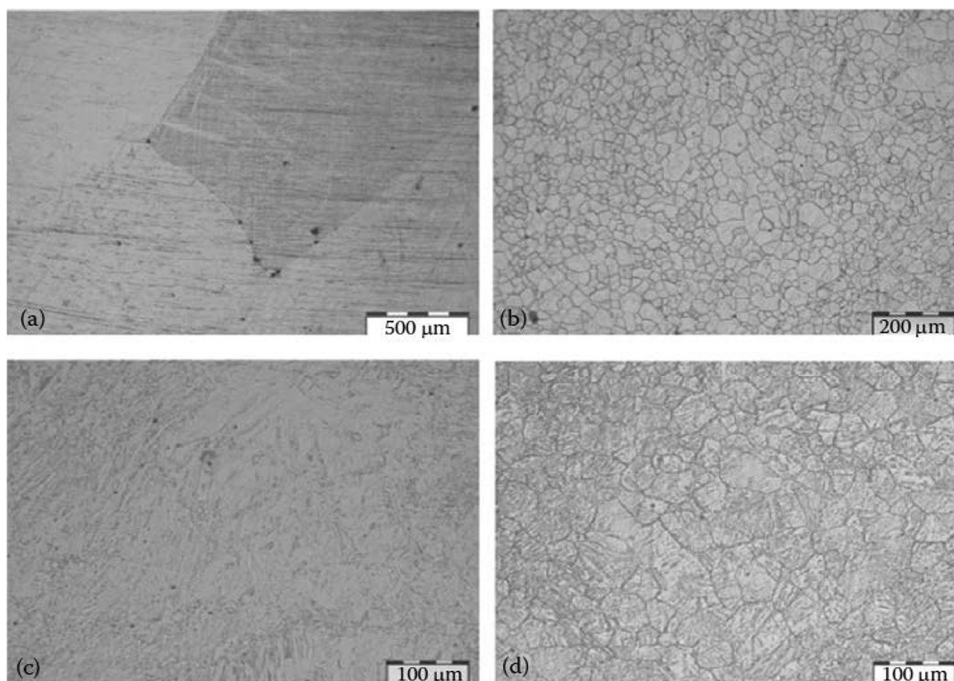


Fig. 13. Optical micrographs of Mg in (a) the as-cast condition, (b) the extruded condition, (c) the as-cast Mg processed by one half turn of HPT, and (d) the extruded Mg processed by one turn of HPT [66–70].

subsequent to more rolling cycles. The precipitation of the apatite layer pertaining to active nucleation sites occurred on the grain boundary areas of the rolled samples which facilitates the corrosion protection [77]. The homogeneous microstructure with finer grains were observed in the Mg-6Zn-1Y-0.6Ce-0.6Zr

alloy [78] was fabricated by the reciprocating extrusion (RE) process. The increase in extrusion passes revealed the reduction in grain size to $\sim 1.2 \mu\text{m}$ and higher yield strength of about 332 MPa with high ductility. Mg-3Ca alloy ribbons [68] were fabricated by a melt-spinning process at various wheel-rotating

Table 7

Mechanical properties of Mg alloys fabricated through different processing techniques [71–75].

Processing route	Grain size (μm)	UTS (MPa)	YS (MPa)	Elongation (%)
Powder metallurgy + Extruded	–	320	280	2
Extruded	43	167	55	18
Extruded + Screw rolling	2–15	177–205	109–146	7–15
Extruded + Screw rolling	2–3	205	146	7
As-cast	>100	58	–	7.2
As-cast	–	86	24	4.8
Extruded + annealing	9–35	162–199	82–124	7–12
Cast-ECAE Mg-2Zn-0.5Ca/1 β -TCP				

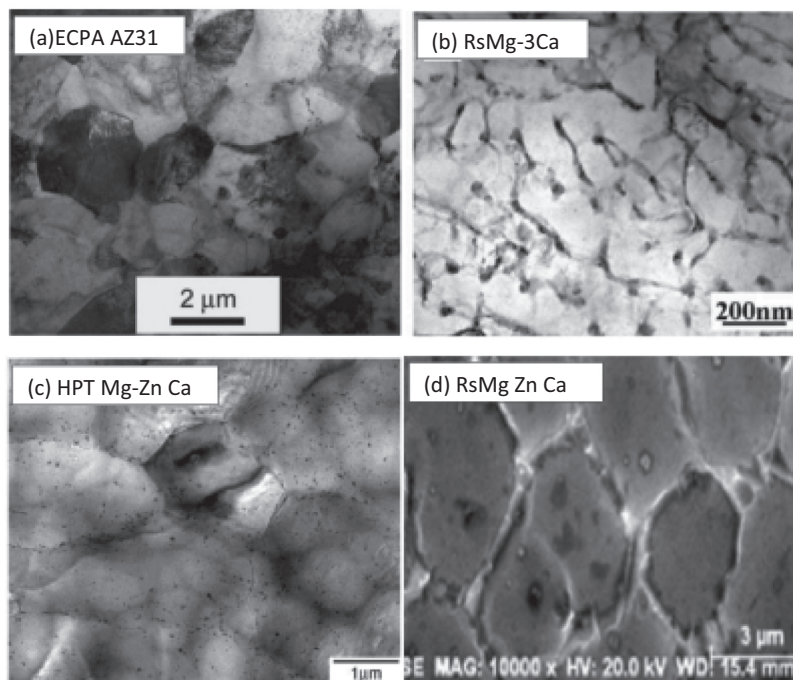


Fig. 14. (a) ECPA AZ31, (b) RS Mg-3Ca, (c) HPT MgZnCa, and (d) RS MgZnCa [66–70].

speeds at the rate of 15, 30, and 45 m/s. The surface area ratio of the secondary phase Mg_2Ca in Mg matrix improved the microstructural and electrochemical properties. With the increase in rotating speed, thinning of Mg-Ca ribbons was observed. It exhibits good cytocompatibility compared with as cast Mg-3Ca alloy. The different cooling techniques such as cooling with thermal insulation, exposed to air and liquid nitrogen were adopted during the solidification of Mg-Zn-Ca [79] alloys respectively. The grain refinement was observed with the higher cooling rates. The grain size was reduced from 100 to 3 μm . The super saturation and homogeneous distribution of alloying elements increased the corrosion resistance. Mg-2Zn-0.24Ca was prepared by high pressure torsion treatment (HPT) [69]. The precipitation of secondary phase particles is observed in the interior of grains rather than grain boundaries. The reduction in grain size was noticed from 100 μm to only 1.2 μm . The uniform corrosion behavior was observed in HPT alloy when the alloy is immersed in simulated body fluid (SBF). The grain refinement was evaluated in AZ31 alloy by equal channel angular pressing (ECAP) with or without the application of back pressure (BP) [80]. The reduction in grain size from 8.5 μm to 1.78 μm , improvement in strength and corrosion resistance was observed in after four passes of ECAP with back pressure of 125 MPa.

7. Bio-perspectives and challenges of Mg alloys

The mechanical properties, biocompatibility, and corrosion resistance properties of the Mg alloys are benefited from the alloying elements. Until now, the vital elements, such as Ca, Zn, Mn, Sr, Sn and Ag etc., were reported to fabricate the degradable alloy system for biomedical applications. Mg-Ca-based

alloys possess inherent biocompatibility and mechanical property closer with natural cortical bones. Ca can refine the grain size and improve the strength of Mg due to the formation of thermally stable intermetallic phases. Sr, Zr, Mn, Zn would be the best choices for the development of Mg-Ca alloys. However, the composition of elements would be chosen at a desired level to control the release of alloying elements during degradation period. The addition of Ca to Mg alloys can retard the oxidation rate during the melting process by the formation of a dense calcium oxide film on the surface of the melt and improve the oxidation resistance of the Mg in higher temperature operating conditions. It was noted that a low amount of Ca can increase the mechanical properties and corrosion resistance of Mg alloys. The alloying of Zn in Mg can reduce impurities like Fe and Ni, hence enhancing the tensile strength, hardness, ductility and corrosion resistance. However, higher amount of Zn wt% than the maximum solubility of Mg prone to form pores and eutectic phases reduces the strength.

Very few reports on Mg-Sr system show good biocompatibility. Sr acts as a grain refiner promotes favorable strength. Furthermore, hot/cold working process helps to improve the mechanical property of Mg-Sr alloy and severe plastic deformation techniques are suggested to improve the corrosion resistance. Sn has a high solid solubility over a wide temperature range due to the formation of Mg_2Sn intermetallic precipitates. A low amount of Sn, less than 5%, can improve the tensile strength and ductility. Mg-Ag alloy systems attract more attention for the antibacterial property of Ag, which is desired for implantation surgery. Ag can refine grains in Mg alloys thus improve the mechanical strength and ductility of the alloy. It is noticed that the addition of Ag results in more microgalvanic cells between the α -Mg matrix and the MgAg second phase in

the alloys. The heat-treatment processes are suggested to acquire better mechanical properties. It is found to be challenging but still more promising to develop a biodegradable implant should be one of desired mechanical characteristics, controlled degradation matched with tissue healing rate and good biocompatibility. The mechanical properties primarily depend on the solubility of alloying elements, grain size and distribution of secondary intermetallic phases. So, more attention should be given to the design of alloy system and processing technique. The new processing techniques with ease for the fabrication of Mg implants will also be expected to emerge. This review article presents the potential of Mg alloys for implant applications by using biocompatible alloying elements but still some challenges need to be addressed, such as the control of H₂ gas evolution during degradation and infection. The toxicity of alloying elements is to be identified for new alloy compositions. With the development of soft computation, various simulation techniques can also be applied to anticipate the corrosion and mechanical behavior of the novel Mg alloys before the in vitro and in vivo evaluations.

8. Magnesium based composites

8.1. Introduction

Composite materials may be defined as those materials that consist of two or more fundamentally different components that are able to act synergistically to give properties superior to those provided by either component alone. Composites made of bioinert and bioactive ceramics are produced to achieve two important features, bioactivity and mechanical strength. There is also growing focus on customizing the material properties of bioabsorbable and composite materials with fillers such as bioactive ceramics. Ceramic materials for medical applications are an interesting practical field in obtaining biomaterials for implants. Ceramics that are considered for bio applications are commonly termed bioceramics. These are usually polycrystalline inorganic silicates, oxides, and carbides. They are refractory in nature and possess high compressive strength. Bioceramics can be sub-classified into bioinert, bioactive, and biodegradable materials. Bioinert ceramic materials maintain their physical and mechanical properties even in biological environments. Bioactive materials can be highly wear resistant and tough; these materials undergo stress-induced transformation toughening. Biodegradable materials degrade or are resorbed upon implantation in a biological environment. Bioceramics and phosphates in particular, could be used to manufacture ideal biomaterials, due to their high biocompatibility and bone integration, as well as being the materials most similar to the mineral component of the bones. The important advantages when analyzing bioceramics is their low chemical reactivity being almost totally inert and therefore, biocompatible. However, the first ceramics used in medical applications, alumina (Al₂O₃) and zirconia (ZrO₂), are two types known as inert, and that was the main reason why they began to be employed in implant manufacturing. To be precise, the dominant feature of these two materials is extremely slow reaction kinetics, so that they should be considered as “almost inert”. Obviously, other ceramics

exhibit faster, or even very fast, reaction kinetics. As in any other chemical reaction, the reaction products of a substance with its environment may lead to an undesired result (e.g. corrosion of a metallic material), but chemical transformation of the starting material to the desired final product. This is the case with bioactive ceramics; when in contact with physiological fluids, a chemical reaction towards the production of newly formed bone takes place. The coating of a metallic material with ceramic is a complex process which greatly determines the clinical success, because the quality and endurance of the fixation at the interface largely depend on the purity, particle size, and chemical composition of the coating, thickness of the coating layer and surface morphology of the substrate. An additional benefit obtained when coating a metallic implant with ceramic material is that the ion release from the metallic alloy is greatly reduced. The ceramics act as an efficient barrier that retards the diffusion kinetics of metal ions towards the living body. At present the applications of calcium phosphate ceramics are mainly focused on bone defect filling, both in dental and orthopedic surgery. Hydroxyapatite is also being used to improve the bonding of hip joint prostheses, due to its outstanding biological properties such as toxicity, lack of inflammatory response and absence of fibrous or immunological reactions. Therefore, the filling of bone defects and coating of metallic implants are the two main applications of ceramics used in manufacturing biomaterials. The properties of bioceramics materials are given in Table 8.

8.2. Types of reinforcements

8.2.1. Alumina (Al₂O₃)

An alumina ceramic has characteristics of high hardness and high abrasion resistance. The reasons for the excellent wear and friction behavior of Al₂O₃ are associated with the surface energy and surface smoothness of this ceramic. There is only one thermodynamically stable phase, i.e. Al₂O₃ that has a hexagonal structure with aluminum ions at the octahedral interstitial sites. Abrasion resistance, strength and chemical inertness of alumina have made it to be recognized as a ceramic for dental and bone implants.

8.2.2. Zirconia (ZrO₂)

Zirconia is a biomaterial that has a bright future because of its high mechanical strength and fracture toughness. Zirconia ceramics have several advantages over other ceramic materials due to the transformation toughening mechanisms operating in their microstructure that can be manifested in components made out of them.

8.2.3. Carbon

Carbon is a versatile element and exists in a variety of forms. Unlike metals, polymers and other ceramics, these carbonaceous materials do not suffer from fatigue. However, their intrinsic brittleness and low tensile strength limits their use in major load bearing applications. It is used as biomaterial particularly in contact with blood. Hence it is important to evaluate its blood compatibility.

Table 8
Types of bioceramics and properties.

Bioceramics		
Types	Characteristics	Applications
Alumina (Al_2O_3)	Biocompatible and bioinert High hardness, high strength and abrasion resistance Non adherent fibrous membrane at the interface. Stress shielding	femoral head porous coatings for femoral stems bone screws and plates knee prosthesis
Zirconia (ZrO_2)	High fracture toughness High flexural strength Low young's modulus Bio inert, Biocompatible Non toxic	femoral head, artificial knee, bone screws and plates
Bioglass	Biocompatible, Bioactive Non toxic brittle Cannot be used for load bearing applications	Artificial bone and dental implants
Hydroxyapatite (HAp)	Bioresorbable, bioactive and biocompatible Similar composition to bone Good osteoconductive properties	Femoral knee, femoral hip, tibial components, acetabular cup

8.2.4. Calcium phosphate ceramics (CPC)

It has been known for more than twenty years that ceramics made of calcium phosphate salts can be used successfully for replacing and augmenting bone tissue. The most widely used calcium phosphate based bioceramics are hydroxyapatite (HAP) and β -tricalcium phosphate (β -TCP). Hydroxyapatite has the chemical formula $\text{Ca}_{10}(\text{PO}_4)_6(\text{OH})_2$, the Ca/P ratio being 1.67 and possesses a hexagonal structure. It is the most stable phase of various calcium phosphates. It is stable in body fluid and in dry or moist air up to 1200 °C and does not decompose and has shown to be bioactive due to its resorbable behavior.

8.2.5. Other reinforcements

Si_3N_4 has been used as an orthopedic biomaterial, to promote bone fusion in spinal surgery and to develop bearings that can improve the wear and longevity of prosthetic hip and knee joints. Si_3N_4 is currently being introduced as a biomaterial because it is a hydrophilic negative charged ceramic, which means that blood with nutrients and proteins attach to the material, facilitating bone–cell adherence and incorporation of the material in the surrounding bone.

CNTs have vast prospective in the manufacturing of hard tissue implants, scaffolds, micro catheters, and as substrates for neuronal growth disorders. Titanium and its reinforcements

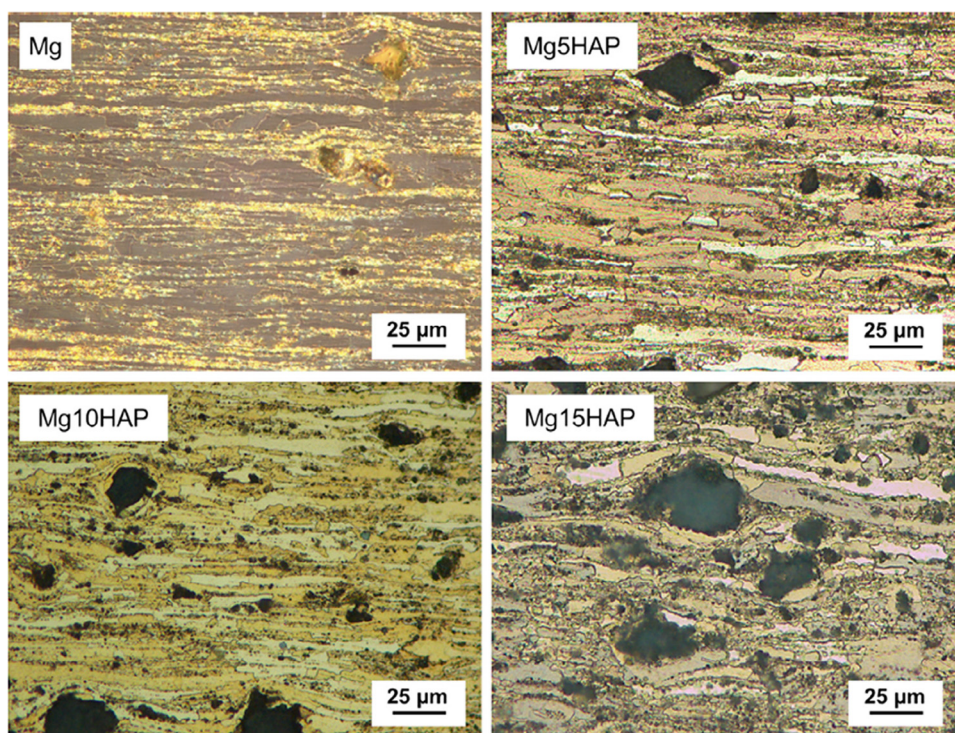


Fig. 15. Optical microscopic images of Pure Mg, Mg-HAP (5, 10, 15 wt %) [81].

(TiB₂, TiC, and TiN) has been a promising biomaterial especially for load-bearing applications due to its biocompatibility, good tribological properties, excellent hardness and high corrosion confrontation.

8.3. Recent trends in magnesium matrix composites

Mg (5, 10, and 15) wt% HAp composites using powder metallurgy (PM) technique followed by hot extrusion was analyzed for its mechanical and microstructural properties. The equiaxed grain structure was revealed and reduction in grain

size was also observed as shown in Fig. 15. XRD studies confirmed small peaks related to HAp [81] as shown in Fig. 16. The maximum hardness and compression strength was observed with the increase in addition of HAp. Mg-5HAP exhibited good corrosion resistance due to the level of porosity and change in intensity of texture. The corrosion penetration rate for Mg-HAP composites are shown in Fig. 17.

Mg-TiO₂ nanocomposites are fabricated using disintegrated melt deposition technique followed by hot extrusion. The grain size was reduced with the addition of TiO₂ (1.98 vol %) in Mg

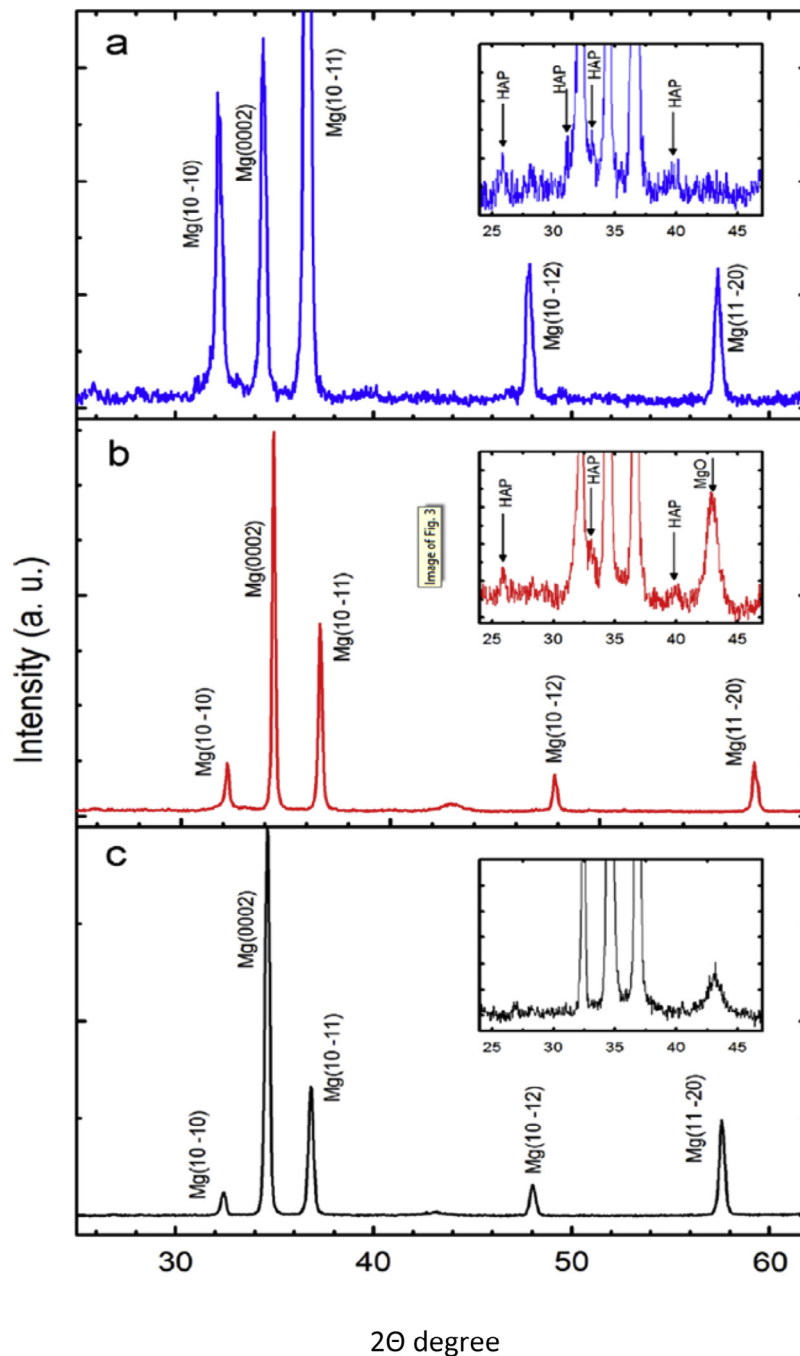


Fig. 16. X-Ray diffraction patterns of (a) Mg-15HAP powder, (b) consolidated Mg-15HAP and (c) consolidated Mg [81].

Table 9
Mechanical and corrosion properties of Magnesium Matrix composites.

Material	Condition	UCS (Mpa)	UTS (MPa)	YS (MPa)	Hardness (HV)	Elongation	I_{corr} (A/cm ²)	Ref
Mg-2Zn-0.5Ca/1 β -TCP	Normal Casting Mg-2Zn-0.5Ca then remelting to add TCP				789.9 \pm 8.8 vickers micro hrdness		789.9 \pm 8.8 CR* (0–36 h) mgcm ⁻² h ⁻¹	[85]
β -Ca ₃ (PO ₄) ₂ /Mg-Zn	PM + extrusion			183			7 (μ A·cm ⁻²)	[86]
Mg-Bredigite 40 vol%	PM + extrusion		190		73			[87]
a) Mg60	As-cast	580					~	[88]
b) Mg67		440						
c) Mg60T40		800						
d) Mg67T40		700						
a) Pure Mg		174 \pm 7			46 \pm 3			[89]
b) Mg0.5SiO ₂		220 \pm 2			53 \pm 1			
c) Mg1SiO ₂		03 \pm 10			62 \pm 4			
d) Mg2SiO ₂		207 \pm 3			69 \pm 2			
BG-5/Mg	PM				42.5			[90]
BG-10/Mg					47.5			
BG-15/Mg					49			
Mg-Mn-Zn-Zr	PM						1.62 $\times 10^{-4}$	[91,92]
Mg-Mn-Zn-Zr-5HA							3.39 $\times 10^{-4}$	
Mg-Mn-Zn-Zr-5BG							1.49 $\times 10^{-4}$	
Mg-Mn-Zn-Zr-5HA microcrystalline Mg							2.43 $\times 10^{-4}$ 3.34 $\times 10^{-4}$	
Mg-CS 10 wt %		178						[93]
Mg-CS 20 wt %		235						
Mg-CS 30 wt %		232						
Mg-CS 40 wt %		212						
Mg-CS 50 wt %		170						
Pure Mg	As-cast	20–115	108.3 \pm 3.1			27.8 \pm 0.8 9.6		
Pure Mg	PM + extrusion	340						[81]
Mg-5HAp	PM + extrusion	222						
Mg-10HAp	PM + extrusion	219						
Mg-15HAp	PM + extrusion	216						
Mg-0.58(vol%)TiO ₂		285	128		58	10		[83]
Mg-0.97(vol%)TiO ₂		278.4	154		61	10.8		
Mg-1.98(vol%)TiO ₂		297	165		64	11.5		
Mg-2.5(vol%)TiO ₂		305.5	170		68	10		
Mg-HA-TiO ₂ -Mgo		253				9.8	255	
AZ91-10FA	PM				86	5.78	7.4 $\times 10^{-5}$	[84]
AZ91-20FA	PM				93	5.32	2.3 $\times 10^{-6}$	
AZ91-30FA	PM				105	4.51	3.5 $\times 10^{-7}$	

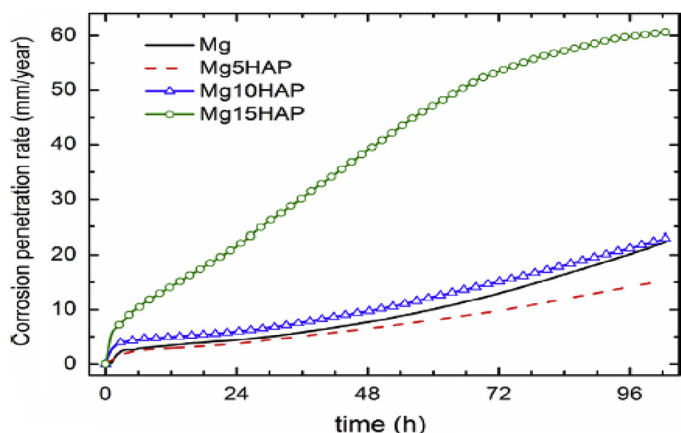


Fig. 17. Corrosion penetration rate for Mg-HAp composites immersed 100 h in PBS solution [81].

matrix. With addition of 2.5 vol. % TiO₂, proof stress, the ultimate tensile strength and fracture strain of pure magnesium increased by ~37%, ~9% and ~31% respectively with the addition of 2.5 vol % of TiO₂. The optical microstructure of Mg-TiO₂ composites and cleavage mode of fractures [82] are shown in Figs. 18 and 19.

Mg MMC prepared by mechanical alloying and annealing at 500 and 630 °C of Mg-HA-TiO₂-MgO mixture. Mg-matrix bio nanocomposite consisting of Mg-substituted HA, Mg₃(PO₄)₂, CaTiO₃, MgTiO₃ and Mg(OH)₂ phases. Annealing at 500 °C for 1 hr, MgTiO₃ formed in the milled samples. Annealing at 630 °C for 1 hr, more HA was decomposed, and thus, greater amounts of the Mg₃(PO₄)₂, Mg(OH)₂ and CaTiO₃ phases were obtained. Corrosion tests in SBF solution revealed that increasing the milling times and HA amounts leads to a decrease in the corrosion rate [83]. The effect of reinforcing various amount of Flurapatite (FA) nano particles (10, 20, 30 wt%) on mechanical and bio-corrosion behavior

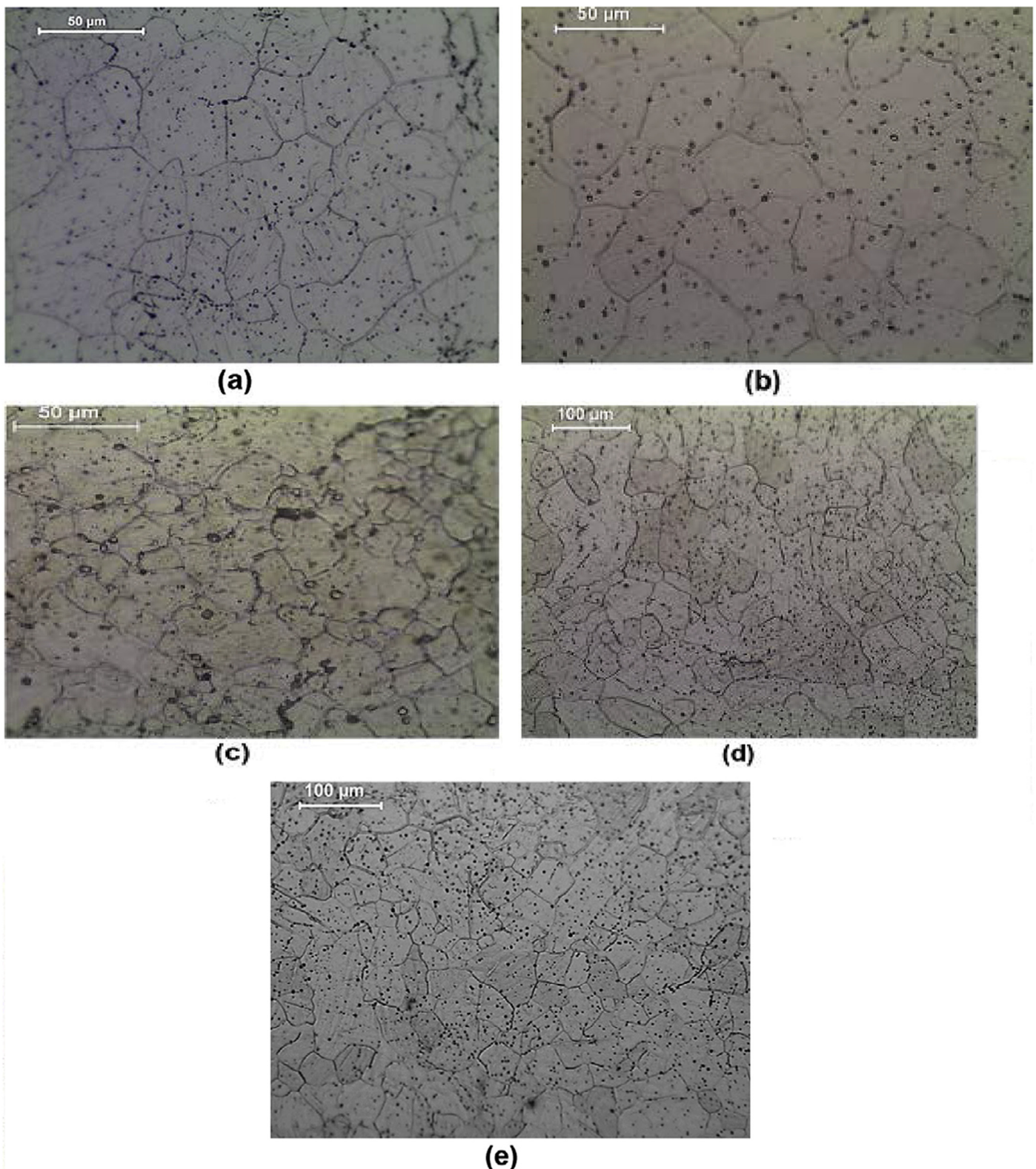


Fig. 18. Optical Microscopic images of (a) pure magnesium, (b) Mg0.58TiO₂, (c) Mg0.97TiO₂, (d) Mg1.98TiO₂ and (e) Mg2.5TiO₂ [82].

on AZ91 Mg alloy was analyzed. With the increase in the amount of FA reinforcements, the reduction in ductility was noticed due to the limiting effect of deformation of matrix caused by the dislocation movement with twinning. The hardness was increased significantly due to the presence

of hard ceramic particles at the interface obstruct the deformation during indentation. The improvement in corrosion resistance was observed with the increase in the amount of FA in AZ91 Mg alloy and SEM micrographs of corroded AZ91-FA composites [84] are shown in Fig. 20.

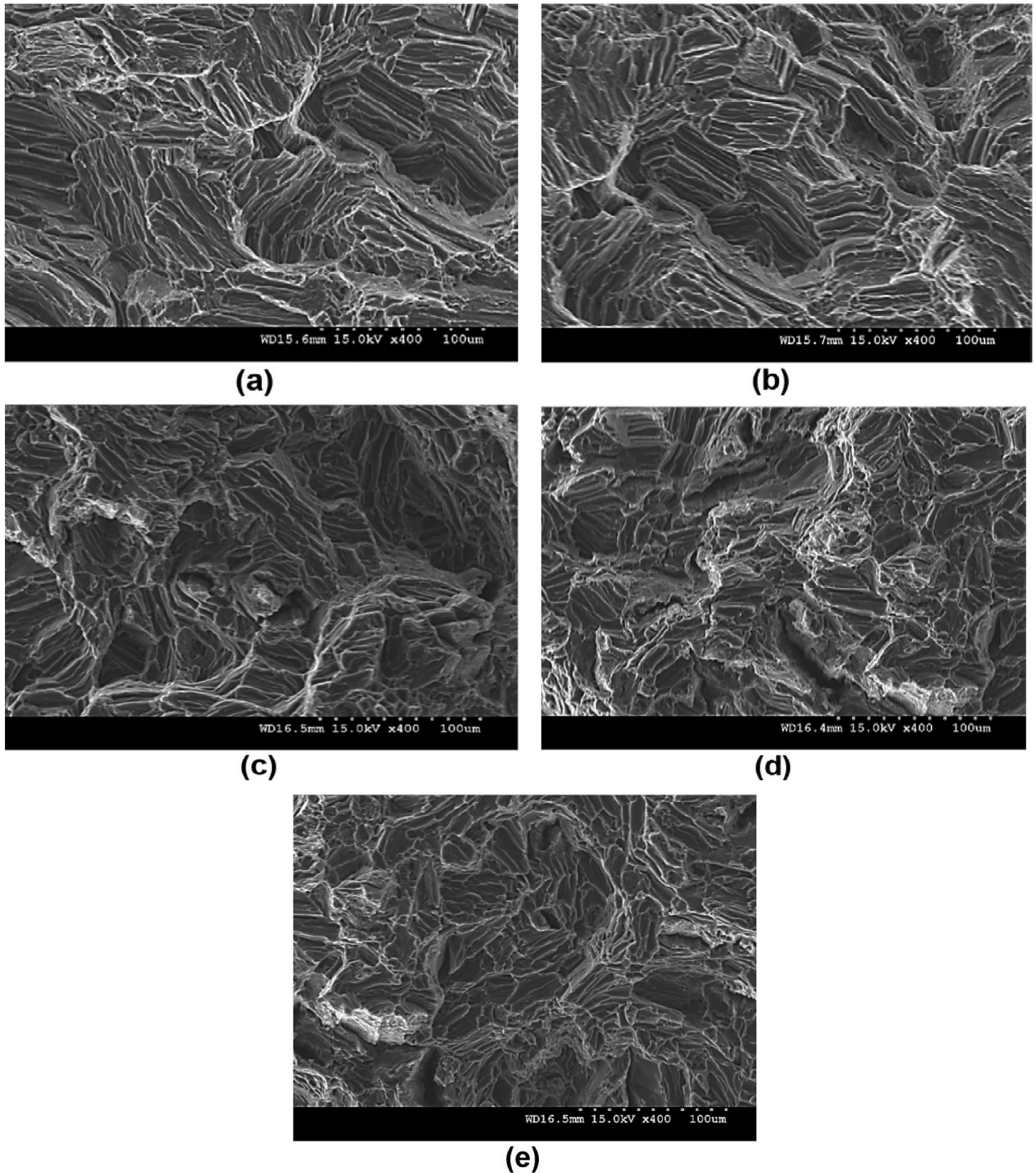


Fig. 19. Tensile fractographs of (a) pure magnesium, (b) Mg_{0.58}TiO₂, (c) Mg_{0.97}TiO₂, (d) Mg_{1.98}TiO₂ and (e) Mg_{2.5}TiO₂ [82].

The corrosion properties of various Mg and Mg alloy matrix composites are given in Table 9. Mg-2Zn-0.5Ca/ β TCP composites are subjected to ECAE exhibited good grain refinement with uniform distribution of β TCP particles in Mg alloy matrix [85] as shown in Fig. 21.

The formation of dense layer of particles and corrosion products together when the composite is immersed in SBF facilitates the bone remodelling [86]. 10% β -Ca₃(PO₄)₂/Mg-6%Zn (wt. %) composites processed by powder metallurgy, hot extrusion followed by heat treatment. The corrosion test

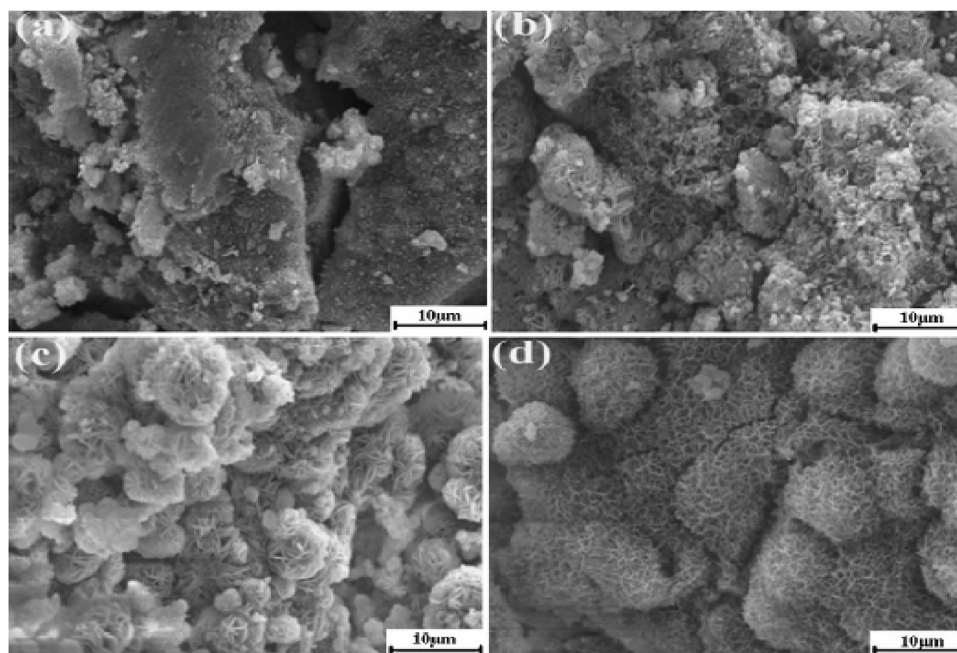


Fig. 20. SEM photomicrographs of (a) AZ91 magnesium alloy, (b) AZ91-10FA, (c) AZ91-20FA, and (d) AZ91-30FA nanocomposites after 72 h immersion time in SBF solution [84].

revealed that formation of protective corrosion layer ($\text{Mg}(\text{OH})_2$, $\beta\text{-Ca}_3(\text{PO}_4)_2$ and HA) on the surface with the addition of $\beta\text{-Ca}_3(\text{PO}_4)_2$, hot extrusion and aging treatment [86] as shown in Fig. 22.

Mg-40 vol% bredigite composites processed by powder metallurgy possess strength closer to the cortical bone. The optical micrographs of pure Mg and Mg-40Bredigite are shown in Fig. 23. The bio-degradation rate of Mg was reduced 24 times with the addition of bredigite particles in the matrix [87].

Mg₆₀Zn₃₅Ca₅ BMGC containing 40 vol% of Ti particles exhibited more uniform lower degradation rate compared with that of the other composites expressing that the Mg₆₀Zn₃₅Ca₅ BMGC releases its Mg ions uniformly and slowly [88] as shown in Fig. 24.

Mg-20 Vol% SiO_2 composites showed grain refinement with good mechanical properties closer to the bone with good damping characteristics favorable for implant applications [89]. The addition of pearl powder (PP) in Mg matrix slow down the degradation rate of Mg [94] promotes the cell adhesion and proliferation suitable for bone implants. The degradation behaviour of Mg-XPP (6, 10, 14 wt%) are depicted in Fig. 25. The addition of bioglass in Mg improves the mechanical properties and reduce the hydrogen evolution and exhibits biocompatibility [95]. HA particles may act as an effective heterogeneous nuclei for $\alpha\text{-Mg}$ phase during the solidification of the Mg-Zn-Zr alloy [90] possibly enhances the nucleation rate greatly limits the grain growth are shown in Fig. 26.

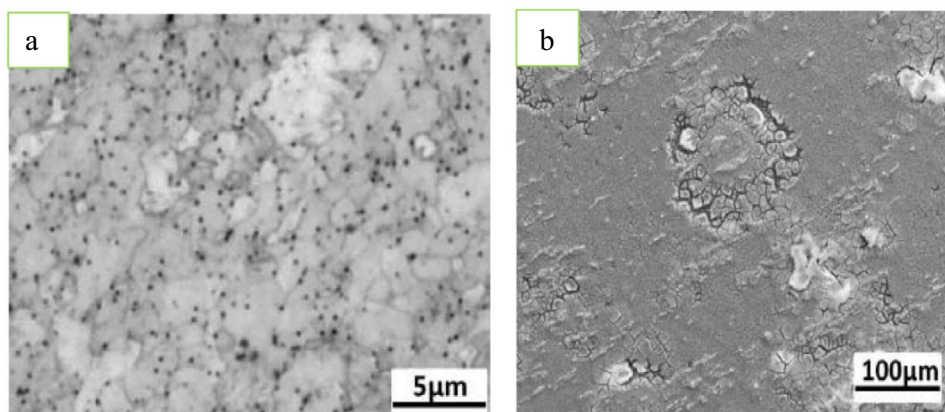


Fig. 21. (a) Optical micrographs of Mg-2Zn-0.5Ca/ β TCP composites subjected to 4 pass ECAE (b) SEM microstructure of corroded Mg-2Zn-0.5Ca/ β TCP composites subjected to 4 pass ECAE [85].

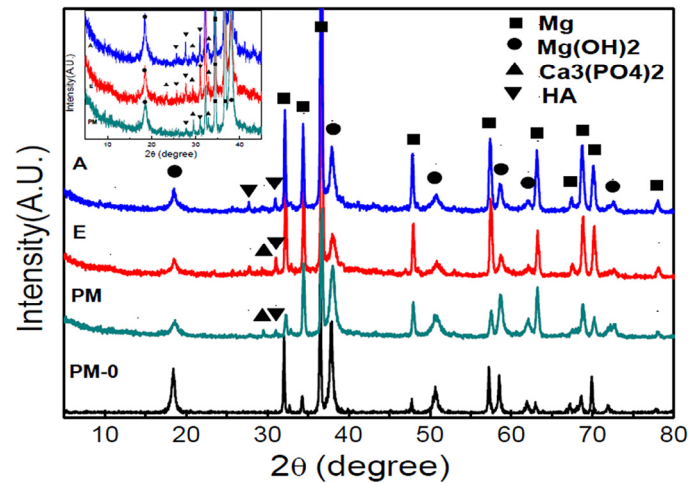


Fig. 22. XRD patterns of the β - $\text{Ca}_3(\text{PO}_4)_2$ /Mg-Zn composites and Mg-Zn alloy after 72 hours immersion in Ringer's solution [86].

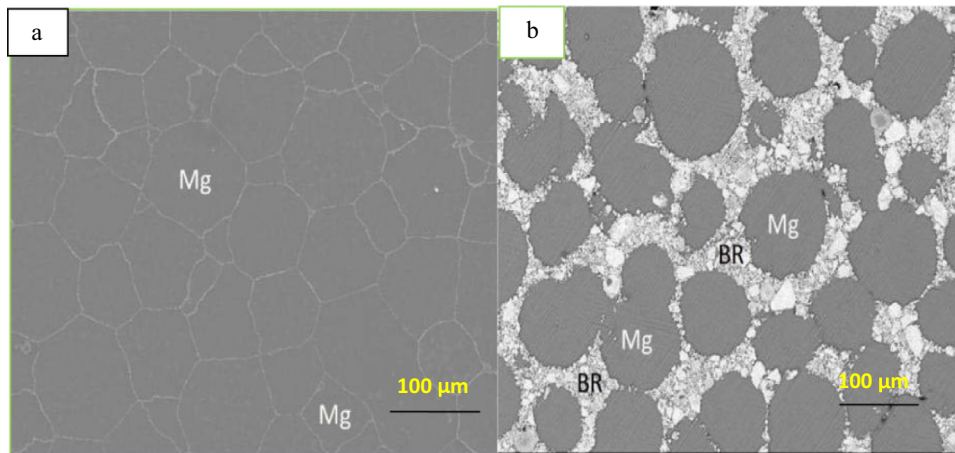


Fig. 23. Optical micrograph of (a) pure Mg (b) Mg-40Bredigite [87].

8.4. Bio-perspectives and challenges on Mg based composites

There continues to be significant interest in developing new biomaterials with favorable mechanical and degradation properties for orthopedic implant applications. The review shows the recent progress in development of Mg/Mg alloy composites for orthopedic biomaterials. The grain refinement and precipitation of secondary phases in Mg matrix plays a very significant role in improving the mechanical and corrosion properties of Mg. The mechanical and degradation behavior of Mg/Mg alloys composites are mainly dependent on the alloying elements, reinforcements and processing techniques. The extensive research is very much required in the development of Magnesium matrix composites. The optimal alloying/reinforcement of Mg based bio-composites is to be found out for favorable orthopedic applications. The ability to translate in vitro evaluations, animal studies, and pilot clinical studies to larger scale use will help determine the viability of many of these biomaterials from a safety and effectiveness standpoint to commercialize in a cost effective manner.

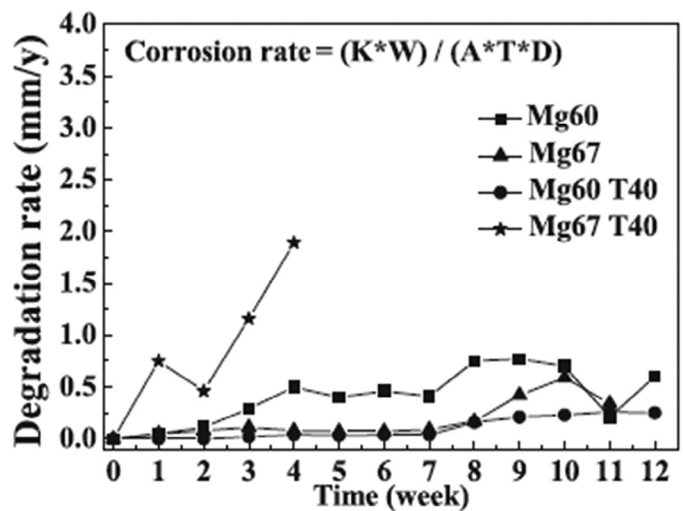


Fig. 24. Degradation rate as a function of immersion time of Mg60Zn35Ca5 BMG, Mg67Zn28Ca5 BMG, Mg60Zn35Ca5 BMGC and Mg67Zn28Ca5 BMGC [88].

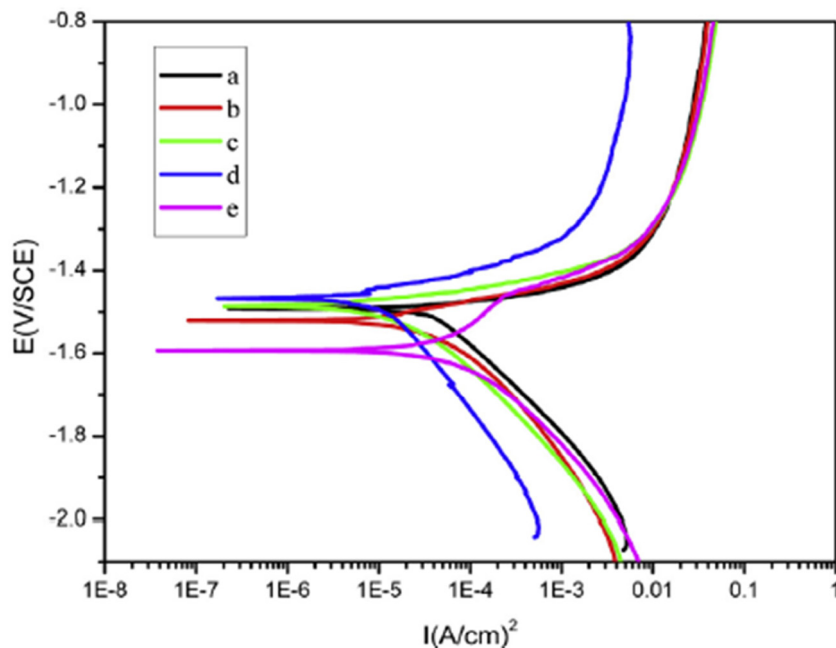


Fig. 25. Potentiodynamic curves of the samples after immersed in simulated body fluid. (a) 100% Mg, (b) Mg-2PP, (c) Mg-6PP (d) 9 Mg-10PP and (e) Mg-14PP [94].

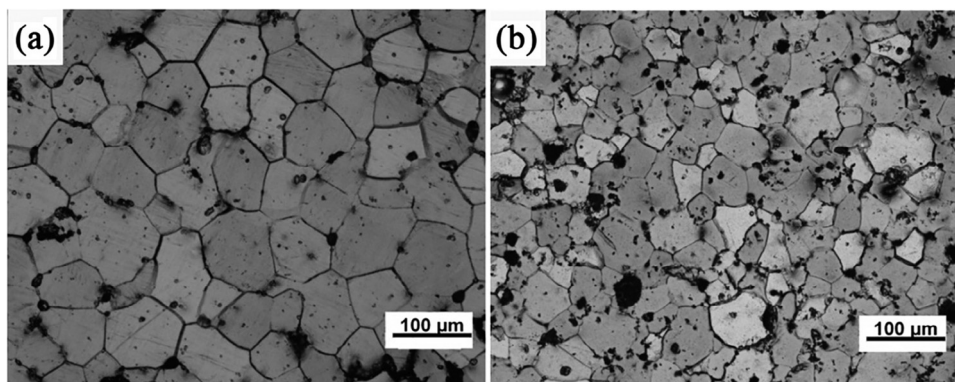


Fig. 26. Optical micrographs of (a) Mg-3Zn-0.8Zr, (b) Mg-3Zn-0.8Zr-1HA [90].

9. Concluding remarks

This review article will help young researchers to choose suitable materials and processing techniques by highlighting the recent trends in the emerging area of Mg based materials for orthopedic implants.

Conflict of interest

There is no conflict of interest.

References

- [1] J.P. DeAngelis, B.D. Browner, A.E. Caputo, J.W. Mast, M.W. Mendes, in: B.D. Browner, A. Levine, J. Jupiter, P. Trafton, C. Krettek (Eds.), *Skeletal Trauma*, 4th ed., W.B. Saunders Company, Philadelphia, 2008.
- [2] F. Witte, I. Abeln, E. Switzer, V. Kaese, A. Meyer-Lindenberg, H. Windhagen, *J. Biomed. Mater. Res. A* 86 (2008) 1041–1047.
- [3] Y. Yun, Z. Dong, D. Yang, M.J. Schulz, V.N. Shanov, S. Yarmolenko, et al., *Mater. Sci. Eng. C* 6 (2009) 1814–1821.
- [4] H.S. Brar, M.O. Platt, M. Sarntinoranont, P.I. Martin, M.V. Manuel, *JOM* 61 (2009) 31–34.
- [5] H.Y. Lopez, D.A. Cortes-Hernandez, S. Escobedo, D. Mantovani, *Key Eng. Mater.* 309–311 (2006) 453–456.
- [6] W.F. Ng, K.Y. Chiu, F.T. Cheng, *Mater. Sci. Eng. C* 6 (2010) 898–903.
- [7] K.Y. Chiu, M.H. Wong, F.T. Cheng, H.C. Man, *Surf. Coat. Technol.* 3 (2007) 590–598.
- [8] The American Foundry Society Technical Dept., *Magnesium Alloys*, The American Foundry Society, Schaumburg, IL, 2006.
- [9] A.M. Richards, W. CNathan, A. KTrevor, M.B. Stephen, C. Simon, *J. Osteoporos.* 2010 (2010) 504078.
- [10] M.M. Avedesian, H. Baker, *Magnesium and Magnesium Alloys*, ASM International, Materials Park, OH, 1999.
- [11] E.F. Emley, *Principles of magnesium technology*, Pergamon Press, 1966.
- [12] N.T. Kirkland, I. Kolbeinsson, T. Woodfield, G.J. Dias, M.P. Staiger, *Mater. Sci. Eng. B* 176 (2011) 1666–1672.
- [13] N.T. Kirkland, I. Kolbeinsson, T. Woodfield, G.J. Dias, M.P. Staiger, *Mater. Lett.* 64 (2010) 2572–2574.
- [14] N.T. Kirkland, I. Kolbeinsson, T. Woodfield, G.J. Dias, M.P. Staiger, *Int. J. Mod. Phys. B* 23 (2009) 1002–1008.

- [15] H. Kuwahara, Y. Al-Abdullat, M. Ohta, S. Tsutsumi, K. Ikeuchi, N. Mazaki, et al., *Mater. Sci. Forum* 350–351 (2000) 349–358.
- [16] K.G. Davis, W.S. Marras, T.R. Waters, *Clin. Biomech. (Bristol, Avon)* 13 (1998) 141–152.
- [17] D. Williams, *Med. Device Technol.* 17 (2006) 9–10.
- [18] F. Witte, N. Hort, C. Vogt, S. Cohen, K.U. Kainer, R. Willumeit, et al., *Curr. Opin. Solid State Mater. Sci.* 12 (2008) 63–72.
- [19] N. Li, Y. Zheng, *J. Mater. Sci. Technol.* 29 (2013) 489–502.
- [20] G.E.J. Poinern, S. Brundavanam, D. Fawcett, *Am. J. Biomed. Eng.* 2 (2012) 218–240.
- [21] X.N. Gu, Y.F. Zheng, Y. Cheng, S.P. Zhong, T.F. Xi, *Biomaterials* 30 (2009) 484–498.
- [22] Y.J. Chen, Y.J. Li, J.C. Walmsley, S. Dumoulin, P.C. Skaret, H.J. Roven, *Mater. Sci. Eng. A Struct. Mater.* 527 (2010) 789–796.
- [23] Y. Nakamura, Y. Tsumura, Y. Tonogai, T. Shibata, Y. Ito, *Fundam. Appl. Toxicol.* 37 (1997) 106–116.
- [24] M.P. Staiger, A.M. Pietak, J. Huadmai, G. Dias, *Biomaterials* 27 (2006) 1728–1734.
- [25] A. Purnama, H. Hermawan, J. Couet, D. Mantovani, *Acta Biomater.* 6 (2010) 1800–1807.
- [26] C.K. Seal, K. Vince, M.A. Hodgson, *IOP Conference Series: Materials Science and Engineering*, vol. 4, 2009, p. 012011.
- [27] M. Salahshoor, Y.B. Guo, *Materials (Basel)* 5 (2012) 135–155.
- [28] F. Witte, J. Fischer, J. Nellesen, H.A. Crostack, V. Kaese, A. Pisch, et al., *Biomaterials* 27 (2006) 1013–1018.
- [29] B.H. Avedesian, *ASM Specialty Handbook: Magnesium and Magnesium Alloys*, 1999, pp. 12–25.
- [30] G.V. Raynor, *The Physical Metallurgy Of Magnesium and Its Alloys*, Pergamon Press, 1959.
- [31] Q.M. Peng, Y.D. Huang, L. Zhou, N. Hort, K.U. Kainer, *Biomaterials* 31 (2010) 398–403.
- [32] S.D. Persaud, A. McGoron, *J. Biomim. Biomater. Tissue Eng.* 12 (2011) 25–39.
- [33] Z.J. Li, X.N. Gu, S.Q. Lou, Y.F. Zheng, *Biomaterials* 29 (2008) 1329–1344.
- [34] B.P. Zhang, Y. Wang, L. Geng, in: R. Pignatello (Ed.), *Biomaterials-Physics and Chemistry*, In Tech, 2011, pp. 183–204.
- [35] X.N. Gu, X.H. Xie, N. Li, Y.F. Zheng, L. Qin, *Acta Biomater.* 8 (2012) 2360–2374.
- [36] Z. Li, X. Gu, S. Lou, Y. Zheng, *Biomaterials* 29 (2008) 1329–1344.
- [37] N.T. Kirkland, I. Kolbeinson, T. Woodfield, G.J. Dias, M.P. Staiger, *J. Biomed. Mater. Res. B. Appl Biomater* 95 (2010) 91–100.
- [38] W.C. Kim, J.G. Kim, J.Y. Lee, H.K. Seok, *Mater. Lett.* 62 (2008) 4146–4148.
- [39] S. Koleini, M.H. Idris, H. Jafari, *Mater. Des.* 33 (2012) 20–25.
- [40] H. Liu, Y. Chen, Y. Tang, S. Wei, G. Niu, *J. Alloys Compd.* 440 (2007) 122–126.
- [41] D. Zander, N.A. Zumdick, *Corros. Sci.* 93 (2015) 222–233.
- [42] G.F. Yang, Y.C. Kim, H.S. Han, G.C. Lee, H.K. Seok, J.C. Lee, *J. Biomed. Mater. Res. B. Appl Biomater* 103 (2015) 807–815.
- [43] C. Zhao, F. Pan, S. Zhao, H. Pan, K. Song, A. Tang, *Mater. Des.* 70 (2015) 60–67.
- [44] H. Ibrahim, A.D. Klarner, B. Poorganji, D. Dean, A.A. Luo, M. Elahinia, *J. Mech. Behav. Biomed. Mater.* 69 (2017) 203–212.
- [45] L. Yuncang, D.H. Peter, W. Cui'e, *J. Mater. Sci.* 46 (2011) 365–371.
- [46] Y. Wan, G. Xiong, H. Luo, F. He, Y. Huang, X. Zhou, *Mater. Des.* 29 (2008) 2034–2037.
- [47] Y.S. Jeong, W.J. Kim, *Corros. Sci.* 82 (2014) 392–403.
- [48] H.R.B. Rad, M.H. Idris, M.R.A. Kadir, S. Farahany, *Mater. Des.* 33 (2012) 88–97.
- [49] M. Bornapour, N. Muja, D. Shum-Tim, M. Cerruti, M. Pekguleryuz, *Acta Biomater.* 9 (2013) 5319–5330.
- [50] D. Tie, F. Feyerabend, N. Hort, D. Hoeche, K.U. Kainer, R. Willumeit, et al., *Mater. Corros.* 65 (2014) 569–576.
- [51] X. Gu, Y. Zheng, Y. Cheng, S. Zhong, T. Xi, *Biomaterials* 30 (2009) 484–498.
- [52] C. Zhao, F. Pan, S. Zhao, H. Pan, K. Song, A. Tang, *Mater. Sci. Eng. C* 54 (2015) 245–251.
- [53] P.R. Cha, H.S. Han, G.F. Yang, Y.C. Kim, K.H. Hong, S.C. Lee, et al., *Sci. Rep.* 3 (2013) 2367.
- [54] M. Bornapour, M. Celikin, M. Cerruti, M. Pekguleryuz, *Mater. Sci. Eng. C* 35 (2014) 267–282.
- [55] D. Fang, X. Li, H. Li, Q. Peng, *Int. J. Electrochem. Sci.* 8 (2013) 2551–2565.
- [56] H.R. Bakhsheshi-Rad, M.R. Abdul-Kadir, M.H. Idris, S. Farahany, *Corros. Sci.* 64 (2012) 184–197.
- [57] P. Yin, N.F. Li, T. Lei, L. Liu, C. Ouyang, *J. Mater. Sci. Mater. Med.* 24 (2013) 1365–1373.
- [58] Y. Lu, A.R. Bradshaw, Y.L. Chiu, I.P. Jones, *Mater. Sci. Eng. C* 48 (2015) 480–486.
- [59] S.A. El Hallem, I. Ghayad, M. Eisaa, N. Nassif, M.A. Shoeib, H. Soliman, *Int. J. Electrochem. Sci.* 9 (2014) 2005–2015.
- [60] H. Li, Q. Peng, X. Li, K. Li, Z. Han, D. Fang, *Mater. Des.* 58 (2014) 43–51.
- [61] E. Zhang, D. Yin, L. Xu, L. Yang, K. Yang, *Mater. Sci. Eng. C* 29 (2009) 987–993.
- [62] H.S. Brar, J. Wong, M.V. Manuel, *J. Mech. Behav. Biomed. Mater.* 7 (2012) 87–95.
- [63] M.B. Kannan, R.S. Raman, *Biomaterials* 29 (2008) 2306–2314.
- [64] A. Zakiyuddin, K. Lee, *J. Alloys Compd.* 629 (2015) 274–283.
- [65] E. Zhang, L. Yang, *Mater. Sci. Eng. A Struct. Mater.* 497 (2008) 111–118.
- [66] X.G. Qiao, Y.W. Zhao, W.M. Gan, Y. Chen, M.Y. Zheng, K. Wu, et al., *Mater. Sci. Eng. A Struct. Mater.* 619 (2014) 95–106.
- [67] Z. Zuberova, L. Kunz, T. Lamark, Y. Estrin, M. Janeccek, *Metall. Mater. Trans. A* 38 (2007) 1934–1940.
- [68] X.N. Gu, X.L. Li, W.R. Zhou, Y. Cheng, Y.F. Zheng, *Biomed. Mater.* 5 (2010) 035013.
- [69] J.H. Gao, S.K. Guan, Z.W. Ren, Y.F. Sun, S.J. Zhu, B. Wang, *Mater. Lett.* 65 (2011) 691–693.
- [70] Z. Xu, C. Smith, S. Chen, J. Sankar, *Mater. Sci. Eng. B* 176 (2011) 1660–1665.
- [71] M.D. Pereda, C. Alonso, L. Burgos-Asperilla, J.A. del Valle, O.A. Ruano, P. Perez, et al., *Acta Biomater.* 6 (2010) 1772–1782.
- [72] M.D. Pereda, C. Alonso, M. Gamero, J.A. del Valle, M. Fernández Lorenzo de Mele, *Mater. Sci. Eng. C* 31 (2011) 858–865.
- [73] M. Díez, H.E. Kim, V. Serebryany, S. Dobatkin, Y. Estrin, *Mater. Sci. Eng. A Struct. Mater.* 612 (2014) 287–292.
- [74] H.F. Sun, C.J. Li, Y. Xie, W.-B. Fang, *Trans. Nonferrous Met. Soc. China* 22 (2012) 445–449.
- [75] Y. Pan, S. He, D. Wang, T. Huang, S. Zheng, P. Wang, et al., *Mater. Sci. Eng. C* 47 (2015) 85–96.
- [76] B.R. Sunil, T.S. Kumar, U. Chakkingal, V. Nandakumar, M. Doble, V.D. Prasad, et al., *Mater. Sci. Eng. C* 59 (2016) 356–367.
- [77] S. Nayak, B. Bhushan, R. Jayaganthan, P. Gopinath, R.D. Agarwal, D. Lahiri, *J. Mech. Behav. Biomed. Mater.* 59 (2016) 57–70.
- [78] X. Guo, D. Shechtman, *J. Mater. Process. Technol.* 187 (2007) 640–644.
- [79] Z.C. Xu, C. Smith, S. Chen, J. Sankar, *Mater. Sci. Eng. R* 176 (2011) 1660–1665.
- [80] F.J. Kang, Q. Liu, J.T. Wang, X. Zhao, *Adv. Eng. Mater.* 12 (2010) 730–734.
- [81] R. Del Campo, B. Savoini, A. Muñoz, M.A. Monge, G. Garcés, *J. Mech. Behav. Biomed. Mater.* 39 (2014) 238–246.
- [82] G.K. Meenashisundaram, M.H. Nai, A. Almajid, M. Gupta, *Mater. Des.* 65 (2015) 104–114.
- [83] S.Z. Khalajabadi, M.R.A. Kadir, S. Izman, M. Kasiri-Asgarani, *Surf. Coat. Technol.* 277 (2015) 30–43.
- [84] M. Razavi, M.H. Fathi, M. Meratian, *Mater. Sci. Eng. A Struct. Mater.* 527 (2010) 6938–6944.
- [85] Y. Huang, D. Liu, L. Anguilano, C. You, M. Chen, *Mater. Sci. Eng. C* 54 (2015) 120–132.
- [86] Y. Yan, Y. Kang, D. Li, K. Yu, T. Xiao, Y. Deng, et al., *Mater. Sci. Eng. C* 74 (2017) 582–596.
- [87] S.N. Dezfili, Z. Huan, A. Mol, S. Leeftang, J. Chang, J. Zhou, *Mater. Sci. Eng. C* 79 (2017) 647–660.
- [88] P.-C. Wong, P.-H. Tsai, T.-H. Li, C.-K. Cheng, J.S.C. Jang, J.C. Huang, *J. Alloys Compd.* 699 (2017) 914–920.

- [89] G. Parande, V. Manakari, G.K. Meenashisundaram, M. Gupta, *Int. J. Mater. Res.* 107 (2016) 1091–1099.
- [90] Y. Wan, T. Cui, W. Li, C. Li, J. Xiao, Y. Zhu, et al., *Mater. Des.* 99 (2016) 521–527.
- [91] K. Kowalski, M. Nowak, M. Jurczyk, *Arch. Metall. Mater.* 61 (2016) 1437–1440.
- [92] D. Liu, Y. Liu, Y. Zhao, Y. Huang, M. Chen, *Mater. Sci. Eng. C* 77 (2017) 690–697.
- [93] Z. Huan, C. Xu, B. Ma, J. Zhou, J. Chang, *RSC Adv.* 53 (2016) 47897–47906.
- [94] W.L.E. Wong, M. Gupta, *NanoWorld J.* 2 (4) (2016) 78–83.
- [95] M. He, X. Hua, X. Fan, D. Pan, *J. Alloys Compd.* 663 (2016) 156–165.